ANTIOXIDANTS & REDOX SIGNALING
Volume 27, Number 6, 2017

DOI: 10.1089/ars.2016.6758

Discoveries

ORIGINAL RESEARCH COMMUNICATION

C-X-C Chemokine Receptor Type 4 Plays a Crucial Role in Mediating Oxidative Stress-Induced Podocyte Injury

Hongyan Mo,[1] Qinyu Wu,[1] Jinhua Miao,[1] Congwei Luo,[1] Xue Hong,[1] Yongping Wang,[1] Lan Tang,[2] Fan Fan Hou,[1] Youhua Liu,[1,3] and Lili Zhou[1]

Abstract

Aims: Oxidative stress plays a role in mediating podocyte injury and proteinuria. However, the underlying mechanism remains poorly understood. In this study, we investigated the potential role of C-X-C chemokine receptor type 4 (CXCR4), the receptor for stromal cell-derived factor 1α (SDF-1α), in mediating oxidative stress-induced podocyte injury.

Results: In mouse model of adriamycin nephropathy (ADR), CXCR4 expression was significantly induced in podocytes as early as 3 days. This was accompanied by an increased upregulation of oxidative stress in podocyte, as demonstrated by malondialdehyde assay, nitrotyrosine staining and secretion of 8-hydroxy-2′-deoxyguanosine in urine, and induction of NOX2 and NOX4, major subunits of NADPH oxidase. CXCR4 was also induced in human kidney biopsies with proteinuric kidney diseases and colocalized with advanced oxidation protein products (AOPPs), an established oxidative stress trigger. Using cultured podocytes and mouse model, we found that AOPPs induced significant loss of podocyte marker Wilms tumor 1 (WT1), nephrin, and podocalyxin, accompanied by upregulation of desmin both *in vitro* and *in vivo*. Furthermore, AOPPs worsened proteinuria and aggravated glomerulosclerosis in ADR. These effects were associated with marked activation of SDF-1α/CXCR4 axis in podocytes. Administration of AMD3100, a specific inhibitor of CXCR4, reduced proteinuria and ameliorated podocyte dysfunction and renal fibrosis triggered by AOPPs in mice. In glomerular miniorgan culture, AOPPs also induced CXCR4 expression and downregulated nephrin and WT1.

Innovation and Conclusion: These results suggest that chemokine receptor CXCR4 plays a crucial role in mediating oxidative stress-induced podocyte injury, proteinuria, and renal fibrosis. CXCR4 could be a new target for mitigating podocyte injury, proteinuria, and glomerular sclerosis in proteinuric chronic kidney disease. *Antioxid. Redox Signal.* 27, 345–362.

Keywords: CXCR4, oxidative stress, podocyte injury

Introduction

PODOCYTES ARE THE HIGHLY SPECIALIZED, terminally differentiated glomerular visceral epithelial cells and play a crucial role in establishing the glomerular filtration barrier. The foot processes of podocytes interdigitate with their neighboring counterparts and form a filtration slit that is connected by slit diaphragm (SD) (34). Increasing evidence demonstrates that podocyte injury often results in the impairment of SD, leading to proteinuria and glomerular sclerotic lesions in various chronic kidney disease (CKD) (12, 17, 39, 57). In diabetic kidney disease or after various glomerular insults, podocyte damage and/or loss often occur in the early stage when endothelial and mesangial cells display little

[1]State Key Laboratory of Organ Failure Research, National Clinical Research Center of Kidney Disease, Division of Nephrology, Nanfang Hospital, Southern Medical University, Guangzhou, China.
[2]Guangdong Provincial Key Laboratory of New Drug Screening, Department of Biopharmaceutics, School of Pharmaceutical Sciences, Southern Medical University, Guangzhou, China.
[3]Department of Pathology, University of Pittsburgh School of Medicine, Pittsburgh, Pennsylvania.

Innovation

Oxidative stress is critical in podocyte injury and glomerulosclerosis. However, the mechanism of oxidative stress-induced podocyte injury remains unclear. The present study demonstrated that the C-X-C chemokine receptor type 4 (CXCR4) mediated advanced oxidation protein products (AOPPs)-aggravated podocyte injury *in vitro* and *in vivo*. CXCR4 induction is dependent on activation of NAPDH oxidase, extracellular signal-regulated kinase (ERK), and p65. Inhibition of CXCR4 reduced oxidative stress, proteinuria, and ameliorated podocyte dysfunction and renal fibrosis triggered by AOPPs in mice. These results suggest that CXCR4 plays a crucial role in mediating oxidative stress-induced podocyte injury, proteinuria, and renal fibrosis.

overt abnormality (5, 11, 44). Therefore, identification of the key factors that regulate podocyte injury would be of great importance in developing rational intervention strategies.

Earlier studies from our laboratory and others have shown that oxidative stress is a key mediator in promoting podocyte injury and proteinuria (13, 45, 53, 54). In advanced oxidation protein products (AOPPs)-overloaded mice, urinary albumin excretion and podocyte depletion are significantly aggravated (54). In podocytes incubated with high glucose, reactive oxygen species (ROS) are elevated dramatically, accompanied by dysregulation of several key podocyte-specific proteins, such as nephrin, podocalyxin, and Wilms tumor 1 (WT1) (9, 10). In mouse model of severe early-onset diabetes, podocyte-specific expression of a potent antioxidant protein, metallothionein (MT), reduces podocyte damage and mitigates diabetic nephropathy (52). Similarly, oxidative stress-triggered podocyte injury appears to be a major culprit in numerous proteinuric kidney diseases, such as hypertension-associated nephropathy and focal segmental glomerulosclerosis (FSGS) (20, 41). However, the underlying mechanisms by which oxidative stress mediates podocyte injury remain to be elucidated.

The C-X-C chemokine receptor type 4 (CXCR4) is the receptor specific for stromal cell-derived factor 1α (SDF-1α), also known as CXC chemokine ligand 12 (CXCL12) (8, 31). CXCR4 is one of the key molecules that tether hematopoietic stem cells to the bone marrow microenvironment. Recent studies have implicated CXCR4 as an important player in rapidly progressive glomerulonephritis (7). In human kidney biopsies, $CXCR4^+$ cells are evident in a variety of glomerular diseases, such as immunoglobulin A nephropathy (IgAN), minimal-change nephrotic syndrome, and FSGS, in which podocyte injury and oxidative stress are common characteristic features (3, 28). These observations prompted us to investigate the potential relationship between CXCR4 and oxidative stress-induced podocyte injury.

In this study, we examined CXCR4 regulation in podocyte injury induced by oxidative stress *in vivo*, *in vitro*, and *ex vivo*. Our results indicate that CXCR4 could play a crucial role in mediating oxidative stress-induced podocyte damage, proteinuria, and renal fibrotic lesions. These findings suggest that CXCR4 could be a new target for mitigating podocyte injury, proteinuria, and glomerular sclerosis in proteinuric CKD.

Results

CXCR4 is upregulated in podocytes in proteinuric CKD

To investigate CXCR4 regulation, we examined its expression by immunohistochemical staining in adriamycin nephropathy (ADR), a model of human FSGS. This model is characterized by an increased oxidative stress, which causes podocyte injury and proteinuria, followed by renal inflammation, glomerulosclerosis, and interstitial fibrosis (48). As shown in Figure 1A, CXCR4 was upregulated predominantly in podocytes in the glomerulus as early as 3 days after injection. Quantitative real-time RT-PCR (qRT-PCR) also showed that CXCR4 messenger RNA (mRNA) was upregulated at 3 days after ADR injection, accompanied by the downregulation of podocalyxin (Supplementary Fig. S1; Supplementary Data are available online at www.liebertpub.com/ars), a podocyte apical membrane protein, which is important for sustaining podocyte integrity (32). To further study the role of CXCR4 in oxidative stress-induced nephropathies, we examined the CXCR4 expression in other models of kidney diseases, including remnant kidney model after 5/6 nephrectomy (5/6NX) and chronic infusion of angiotensin II, both of them have been shown to be associated with podocyte injury and increased levels of oxidative stress (24, 45). Consistently, renal expression of CXCR4 was induced in both models as well (Supplementary Fig. S2). Of note, the expression of C-X-C chemokine receptor type 7 (CXCR7), another receptor for SDF-1 (23), was not altered at 3 days after ADR injection and at 6 weeks after 5/6NX (Supplementary Fig. S3), suggesting a potentially specific and predominant role of CXCR4 in the development of oxidative stress-associated nephropathies.

To further establish the relationship between CXCR4 upregulation and podocyte injury, we assessed the expression of CXCR4, nephrin, and desmin proteins by Western blot analyses. As shown in Figure 1B–E, CXCR4 and desmin, a podocyte injury marker, were upregulated, whereas nephrin was downregulated at 3 days after ADR injection. The *de novo* induction of CXCR4 in podocytes was clearly associated with the development of proteinuria in this model (Fig. 1F), suggesting a potential role for CXCR4 in mediating podocyte injury and proteinuria.

To investigate the relevance of CXCR4 upregulation to human kidney diseases, we examined its expression in human kidney biopsies of patients with proteinuric CKD. As shown in Figure 1G, CXCR4 was also expressed in the glomerulus, especially in podocytes, of human kidneys from patients with IgAN, crescent glomerulonephritis, and FSGS. Staining on series sections of human IgAN biopsies confirmed the colocalization of CXCR4 and AOPPs, an oxidative stress marker, predominantly in glomerular podocytes (Fig. 1H), suggesting their close relationship in the pathogenesis of podocyte injury and proteinuria.

CXCR4 induction in podocytes is associated with oxidative stress

To assess the oxidative status of podocytes after ADR injection, we examined the expression of NOX2, a major subunit of NADPH oxidase, by qRT-PCR. As shown in Figure 2A, NOX2 mRNA was induced significantly at 3 days after ADR injection, suggesting an increased oxidative stress. Furthermore,

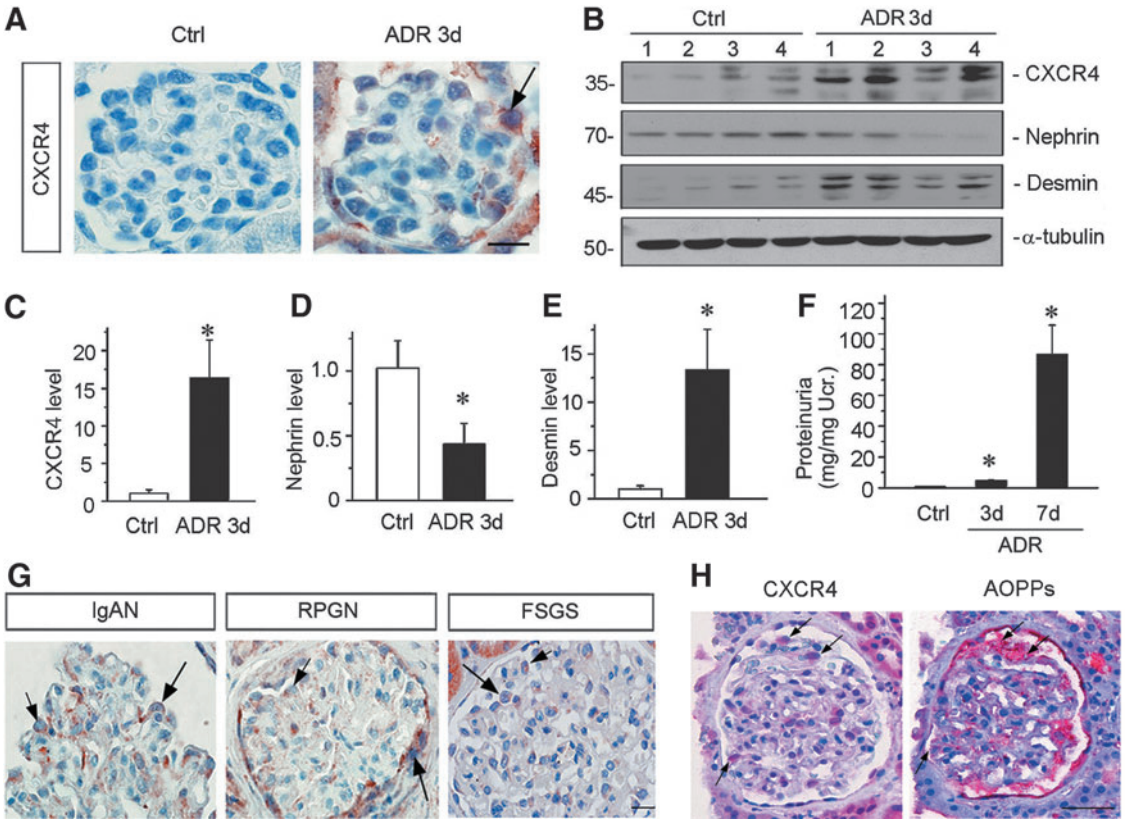

FIG. 1. ***De novo*** **expression of CXCR4 is induced in podocytes after kidney injury. (A)** Immunohistochemical staining demonstrates CXCR4 expression in glomerular podocytes after ADR injury. Three days after ADR (10.5 mg/kg) injection, mice were sacrificed, and paraffin-embedded kidney sections were stained with CXCR4 antibody. *Arrow* indicates positive staining. Scale bar, 15 μm. **(B)** Western blotting analyses of renal expressions of CXCR4, nephrin, and desmin in control and ADR-injected mice. Numbers (1–4) represent different animals in a given group. **(C–E)** Graph presentations show the relative abundance of CXCR4 **(C)**, nephrin **(D)**, and desmin **(E)** protein expression in control (Ctrl) and ADR-treated (ADR 3d) groups. $*p < 0.05$ *versus* normal controls ($n = 5$–6). **(F)** Urinary albumin levels in mice at 3 and 7 days after ADR injection. Data are presented as mg/mg of urinary creatinine. $*p < 0.05$ *versus* normal controls ($n = 5$–6). **(G)** Representative images of CXCR4 staining in human IgAN, RPGN, and FSGS. *Arrows* indicate positive staining in podocytes. Scale bar, 15 μm. **(H)** Colocalization of CXCR4 and AOPPs in the glomeruli of the kidney biopsy from patient with IgAN. Kidney sequential paraffin sections were immunostained for CXCR4 and AOPPs. Colocalizations of CXCR4 and AOPPs in glomerular podocytes are indicated by *arrows*. Scale bar, 40 μm. All full unedited gels for Figure 1 are presented in Supplementary Figure S6. ADR, adriamycin nephropathy; AOPPs, advanced oxidation protein products; CXCR4, C-X-C chemokine receptor type 4; FSGS, focal segmental glomerulosclerosis; IgAN, immunoglobulin A nephropathy; RPGN, rapidly progressive glomerulonephritis.

we detected NOX4, another member of the NOX family of NADPH oxidases (49). Consistent with NOX2, NOX4 was also significantly induced at 3 days after ADR injection (Fig. 2A). We further examined the nitrotyrosine level in the kidneys by immunostaining. As shown in Figure 2B, nitrotyrosine was increased in the glomeruli at 3 days after ADR injection. Double staining with podocyte-specific cytoskeleton protein α-actinin-4 demonstrated that nitrotyrosin was largely colocalized with α-actinin-4 (Fig. 2B). Next, we detected the level of malondialdehyde (MDA), a biomarker of oxidative stress, in the kidney cortex homogenates. As presented in Figure 2C, cortical MDA was increased after ADR injection in a time-dependent manner. Furthermore, urinary 8-hydroxy-2′-deoxyguanosine (8-OHdG), a well-known biomarker of oxidative stress *in vivo* (54), was measured by enzyme-linked immunosorbent assay (ELISA). As shown in Figure 2D, urinary 8-OHdG was time dependently elevated after ADR injection. These results suggest that CXCR4 induction in podocytes after ADR injection is associated with oxidative stress in this model.

AOPPs aggravate podocyte injury, proteinuria, and glomerulosclerosis in vivo

We next investigated whether increased oxidative stress worsens podocyte injury and exacerbates proteinuria in ADR nephropathy. To this end, mice were administered with either ADR alone or ADR plus AOPPs, a known oxidative stress trigger. As shown in Figure 3A and B, urinary albumin level was markedly elevated at 2 weeks after ADR injection, and administration of AOPPs further aggravated proteinuria in this model, as shown by sodium dodecyl sulfate–polyacrylamide gel electrophoresis (SDS-PAGE) analysis of urinary proteins and by ELISA. We further assessed podocyte injury by examining the expression of podocyte-specific markers, including nephrin, WT1, and podocalyxin. As shown in Figure 3C,

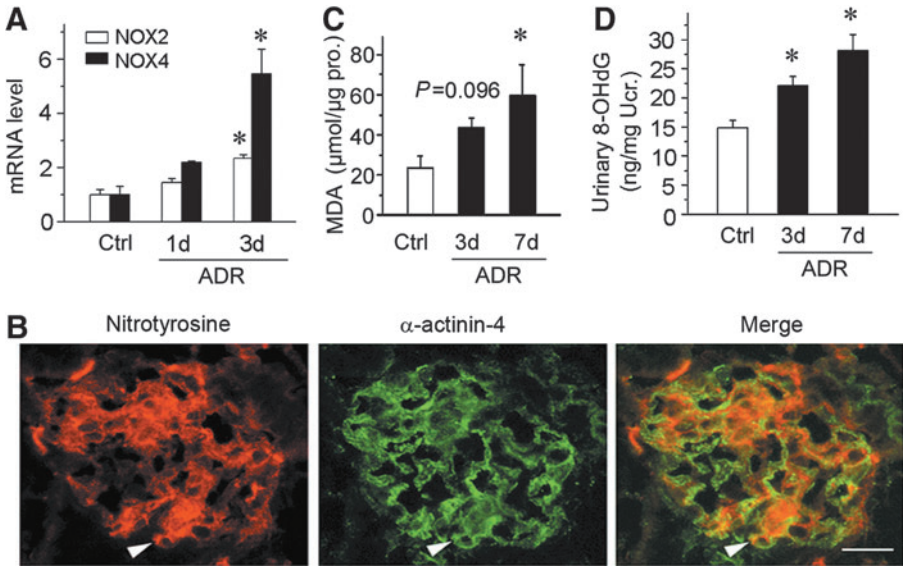

FIG. 2. CXCR4 induction in podocytes is associated with oxidative stress. (A) Graphical representations of the relative abundances of NOX2 and NOX4 mRNA in different groups as indicated. $*p < 0.05$ *versus* normal controls ($n = 5–6$). **(B)** Colocalization of nitrotyrosine and podocyte-specific markers α-actinin-4 in the glomeruli at 3 days after ADR injection. Kidney cryosections were immunostained for nitrotyrosine (*red*) and α-actinin-4 (*green*). *Arrowheads* indicate colocalization of nitrotyrosine and α-actinin-4. Scale bar, 15 μm. **(C)** Graphical representations show MDA levels in renal cortex of mice at 3 and 7 days after ADR injection. $*p < 0.05$ *versus* normal controls ($n = 5–6$). **(D)** Graphical representations show urinary 8-OHdG levels in mice at 3 and 7 days after ADR injection. $*p < 0.05$ *versus* normal controls ($n = 5–6$). 8-OHdG, 8-hydroxy-2′-deoxyguanosine; MDA, malondialdehyde; mRNA, messenger RNA.

immunostaining showed that ADR caused significant down-regulation of nephrin, WT1, and podocalyxin in glomerular podocytes, and administration of AOPPs further aggravated the loss of these proteins. Western blot analyses of kidney lysates also demonstrated that AOPPs significantly accelerated the loss of nephrin and podocalyxin abundances (Fig. 3D, E). Conversely, renal expression of desmin, a podocyte injury marker, was significantly increased in ADR nephropathy, which was further aggravated by AOPPs in this model (Fig. 3D, F).

Because podocyte injury often leads to glomerular sclerotic lesions, we further examined the effect of oxidative stress on glomerular sclerosis in this model. As shown in Figure 3G, periodic acid-Schiff (PAS) staining revealed the characteristic features of glomerular sclerotic lesions, such as mesangial expansion and matrix deposition, glomerular hypertrophy, and capillary collapse. Notably, administration of AOPPs rapidly accelerated ADR nephropathy to proceed into the stage of glomerular sclerosis (Fig. 3G, arrow) whereas ADR alone generally displayed mild glomerular sclerotic lesions at 2 weeks after injection. The extent of glomerular lesions was assessed by a semiquantitative analysis and presented in Figure 3H.

Oxidative stress accelerates renal fibrosis in ADR nephropathy

We further assessed the fibrotic lesions in the kidneys after ADR or ADR plus AOPPs. As shown in Figure 4A, tubular dilation and hyaline casts were detected focally in the kidneys after injection of ADR at 2 weeks. Furthermore, administration of AOPPs aggravated these pathological lesions. Masson's trichrome staining (MTS) revealed substantial renal interstitial fibrosis in the kidneys receiving ADR plus AOPPs at 2 weeks after injections (Fig. 4A, B). Consistently, Western blot analyses of whole-kidney lysates demonstrated that numerous fibrosis-related proteins such as fibronectin, α-smooth muscle actin (α-SMA), and matrix metalloproteinase (MMP-7) were induced at 2 weeks after ADR injection, and administration of AOPPs further enhanced the expression of these proteins (Fig. 4C–F). Immunostaining also indicated that AOPPs aggravated the expression of fibronectin, α-SMA, fibroblast-specific protein 1 (Fsp-1), and collagen type I in this model (Fig. 4G).

Blockade of CXCR4 restores podocyte integrity and protects against proteinuria

To investigate the potential role of CXCR4 in mediating oxidative stress-induced podocyte injury, we injected the mice intraperitoneally with AMD3100, a specific inhibitor of CXCR4 signaling (6, 33). As shown in Figure 5A–D, treatment of AMD3100 restored podocyte integrity in both ADR alone and ADR plus AOPPs groups. Podocyte-specific markers such as nephrin, WT1, and podocalyxin were significantly increased after AMD300 treatment, as assessed by either immunostaining (Fig. 5A) or Western blotting (Fig. 5B–D). We also investigated the therapeutic effects of CXCR4 inhibitor on glomerular sclerotic lesions. As shown in Figure 5A and E, AMD3100 essentially reversed glomerular sclerotic lesions in mice receiving either ADR alone or ADR plus AOPPs injections. Not surprisingly, AMD3100 also reduced urinary albumin levels in mice injected ADR alone or ADR plus AOPPs (Fig. 5F). These data suggest that CXCR4 may play a critical role in mediating podocyte injury induced by oxidative stress.

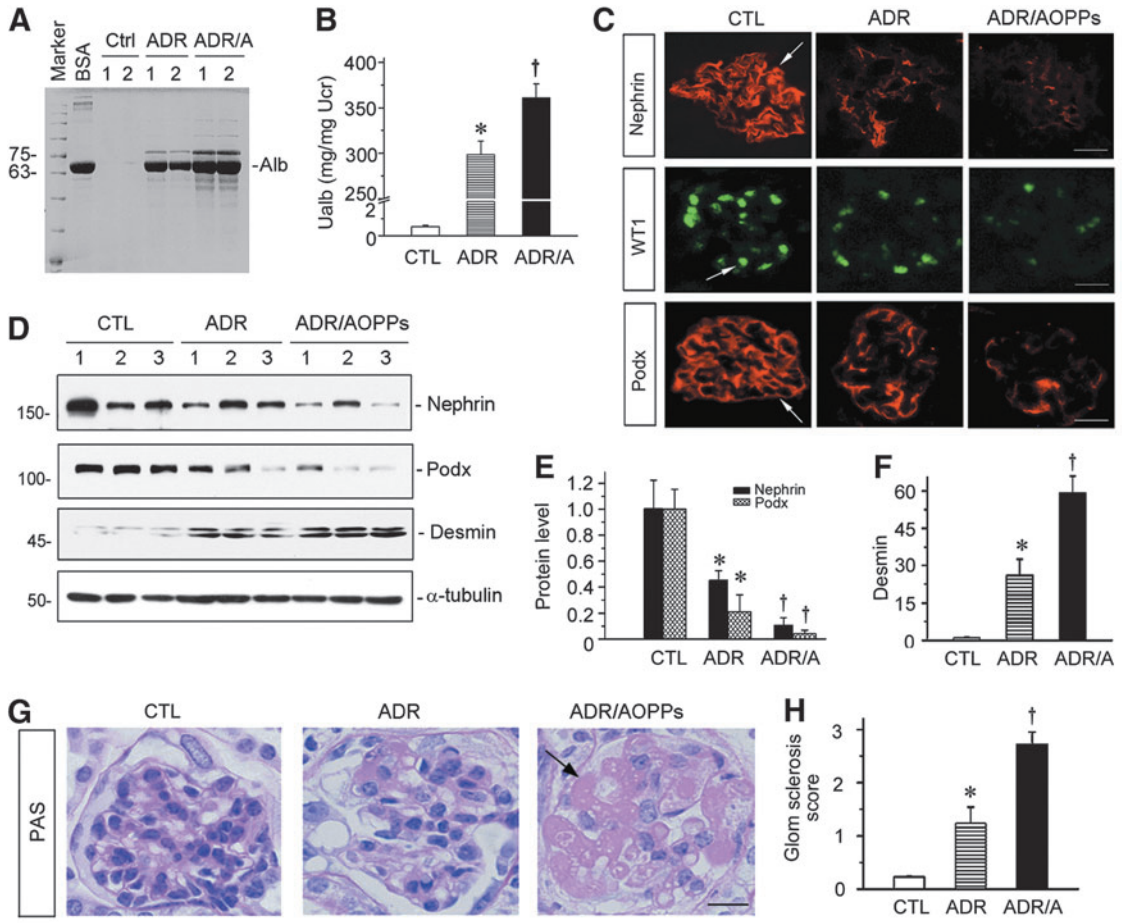

FIG. 3. AOPPs aggravate podocyte injury and accelerate the progression to glomerulosclerosis in ADR nephropathy. **(A)** SDS-PAGE analysis shows the abundance and composition of urinary proteins in different groups of mice at 2 weeks after ADR injection or ADR plus AOPPs. Urine samples after normalization to creatinine were analyzed on SDS-PAGE, with BSA (1 μg) loaded on the adjacent lane. The numbers (1 and 2) indicate each individual, representative animal in a given group. **(B)** Urinary albumin levels in mice at 2 weeks after ADR injection. Urinary albumin is expressed as mg/mg of creatinine. $^{*}p < 0.05$ *versus* normal controls; $^{\dagger}p < 0.05$ *versus* ADR alone ($n = 5$–6). **(C)** Representative images of nephrin, WT1, and podocalyxin staining in different groups as indicated. *Arrows* indicate positive staining. Scale bar, 20 μm. **(D)** Western blot analyses of kidney lysates shows protein abundance of nephrin, podocalyxin, and desmin in different groups. Numbers (1–3) represent different individual animals in a given group. **(E, F)** Graphical representations of nephrin and podocalyxin **(E)** and desmin **(F)** expressions in different groups as indicated. $^{*}p < 0.05$ *versus* normal controls; $^{\dagger}p < 0.05$ *versus* ADR alone ($n = 5$–6). **(G)** Representative micrographs of PAS staining show AOPPs aggravated glomerular sclerosis lesions. *Arrow* indicates sclerotic area. Scale bar, 15 μm. **(H)** Quantitative analyses show glomerular sclerosis score in different groups of mice at 2 weeks after ADR injection or ADR plus AOPPs. $^{*}p < 0.05$ *versus* normal controls; $^{\dagger}p < 0.05$ *versus* ADR alone ($n = 5$ to 6). All full unedited gels for Figure 3 are presented in Supplementary Figure S7. ADR/A, ADR plus AOPPs; BSA, bovine serum albumin; Ctrl, control; PAS, Periodic acid-Schiff; SDS-PAGE, sodium dodecyl sulfate–polyacrylamide gel electrophoresis; WT1, Wilms tumor 1.

Blockade of CXCR4 signaling reduces renal fibrosis

We further investigated the effect of blockade of CXCR4 on renal fibrosis in ADR nephropathy. As illustrated in Figure 6A, MTS exhibited that AOPPs aggravated interstitial collagen deposition and fibrotic lesions, and treatment with AMD3100 substantially reduced renal fibrosis. Similarly, immunostaining for Fsp-1, fibronectin, and collagen I also revealed that blockade of CXCR4 by AMD3100 largely abolished the induction of these proteins in the kidneys (Fig. 6A, arrows). Western blot analyses of whole-kidney homogenate further confirmed that AOPPs aggravated renal fibronectin and α-SMA expression in ADR-treated mice, and AMD3100 treatment inhibited their expression in mice injected with ADR alone or ADR plus AOPPs (Fig. 6B–D).

Oxidative stress augments CXCR4 signaling in ADR nephropathy

To further establish the relationship between oxidative stress and CXCR4 signaling, we examined the regulation of SDF-1α/CXCR4 axis in the kidneys after injections with ADR alone or ADR plus AOPPs. As shown in Figure 7A–C, renal SDF-1α and CXCR4 proteins were markedly induced

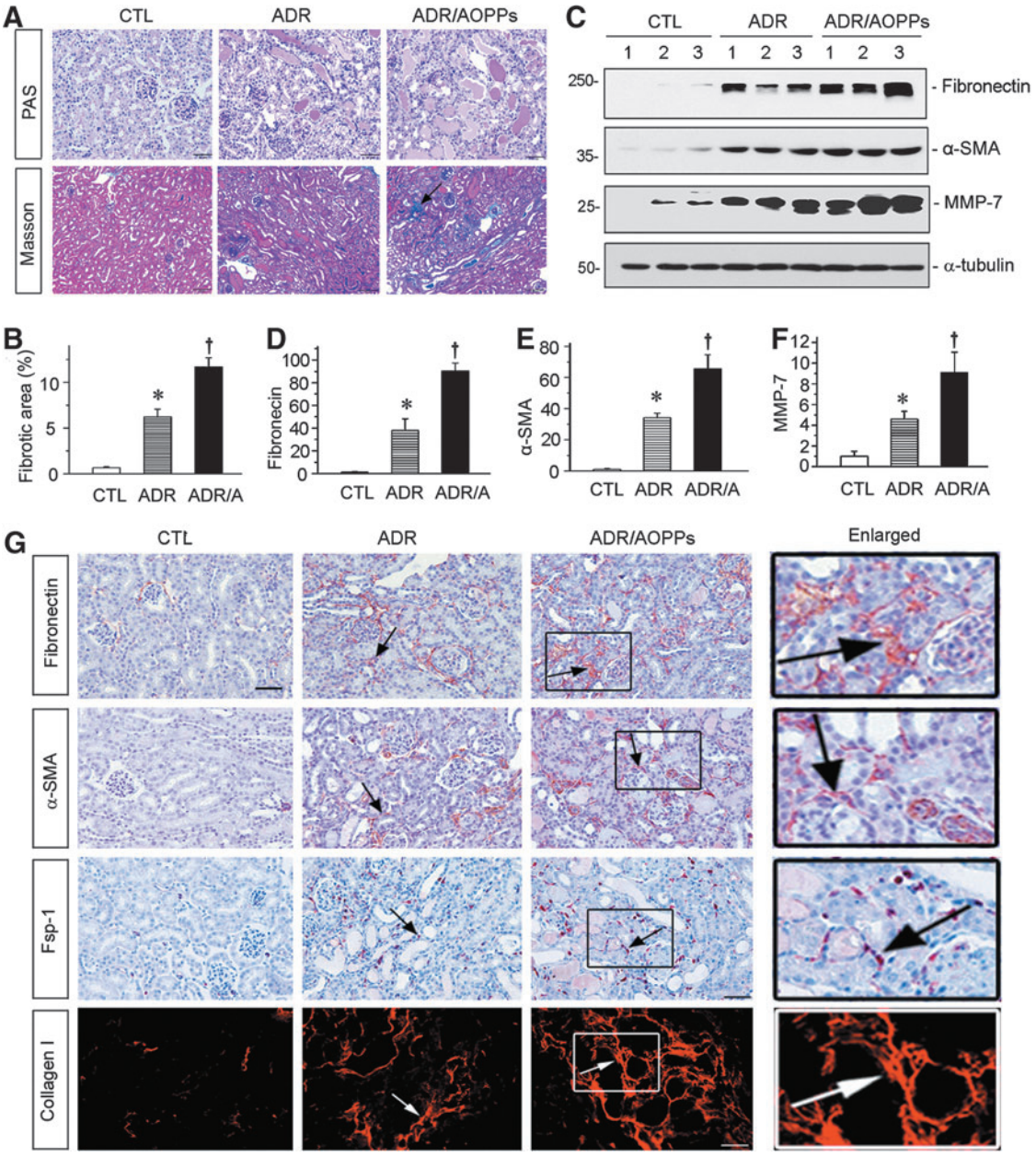

FIG. 4. AOPPs aggravate renal fibrosis in ADR nephropathy. (A) Representative micrographs show that AOPP-accelerated renal interstitial fibrosis. Kidney sections were subjected to PAS and Masson's trichrome staining. *Arrow* indicates positive staining. Scale bar, 50 μm. **(B)** Graphical representation of kidney fibrotic lesions in different groups after quantitative determination. $^{*}p < 0.05$ *versus* normal controls; $^{\dagger}p < 0.05$ *versus* ADR alone ($n = 5$–6). ADR/A indicates ADR plus AOPP group. **(C–F)** Western blot analyses of renal expressions of fibronectin, α-SMA, and MMP-7 in different groups. Numbers (1–3) represent different animals in a given group. Graphical representations of fibronectin **(D)**, α-SMA **(E)**, and MMP-7 **(F)** expressions in different groups as indicated. $^{*}p < 0.05$ *versus* normal controls; $^{\dagger}p < 0.05$ *versus* ADR alone ($n = 5$–6). **(G)** Representative micrographs show fibronectin, α-SMA, Fsp-1, and collagen I expressions in different groups. Paraffin sections were stained with different antibodies. *Boxed areas* are enlarged and presented in the *right column*. *Arrows* indicate positive staining. Scale bar, 50 μm. All full unedited gels for Figure 4 are presented in Supplementary Figure S8. Fsp-1, fibroblast-specific protein 1; MMP-7, matrix metalloproteinase; α-SMA, α-smooth muscle actin.

at 2 weeks after injection of ADR. Administration of AOPPs further aggravated the expression of both SDF-1α and CXCR4 (Fig. 7A–C). Immunohistochemical staining revealed that CXCR4 were specifically induced in glomerular podocytes (Fig. 7D), suggesting a podocyte-specific activation of CXCR4 signaling following oxidative stress.

We sought to explore the upstream mediator responsible for CXCR4 induction in podocytes *in vivo*. Earlier studies implicate the extracellular signal-regulated kinase (ERK) and nuclear factor κB (NF-κB) signaling in regulating CXCR4 expression in tumor cells (15, 25, 38). These observations prompted us to examine their activation in the kidneys after

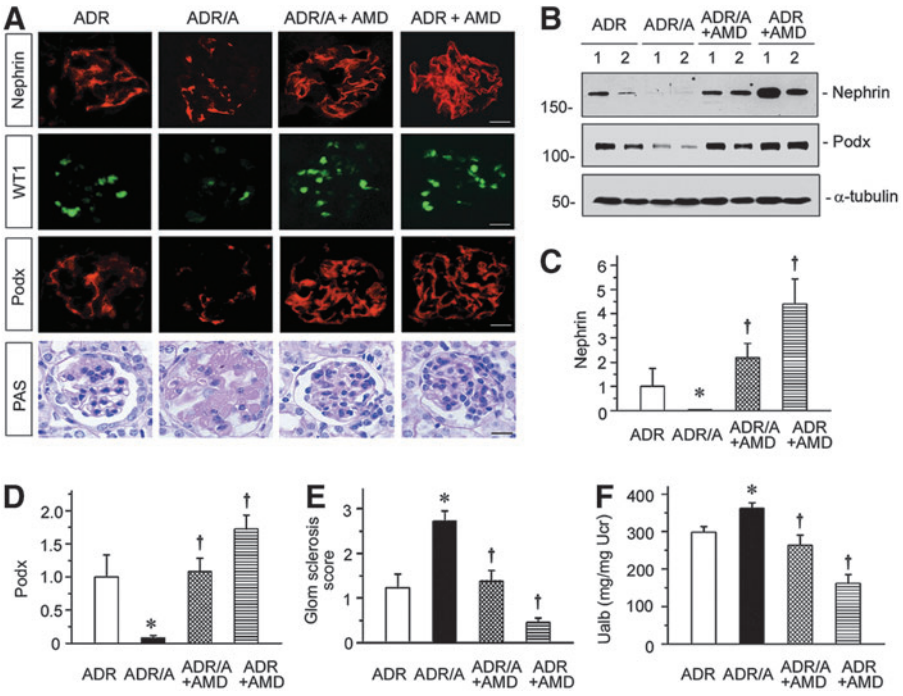

FIG. 5. Blockade of CXCR4 signaling preserves podocyte integrity after oxidative stress. (A) Representative images show immunofluorescence staining of nephrin, WT1, and podocalyxin (Podx) and PAS staining. Scale bar, 20 μm. **(B–D)** Western blotting analyses **(B)** and quantitative graphs of nephrin **(C)** and podocalyxin (Podx) **(D)** in different groups. Numbers (1 and 2) represent different animals in a given group. $^{*}p < 0.05$ *versus* ADR group; $^{\dagger}p < 0.05$ *versus* ADR or ADR plus AOPPs vehicle controls ($n = 5$–6). **(E)** Quantitative analysis shows glomerular sclerosis score in different groups as indicated. **(F)** Urinary albumin levels in different groups of mice. Urinary albumin is expressed as mg/mg of creatinine. $^{*}p < 0.05$ *versus* ADR group; $^{\dagger}p < 0.05$ *versus* ADR or ADR plus AOPPs vehicle controls ($n = 5$–6). All full unedited gels for Figure 5 are presented in Supplementary Figure S9.

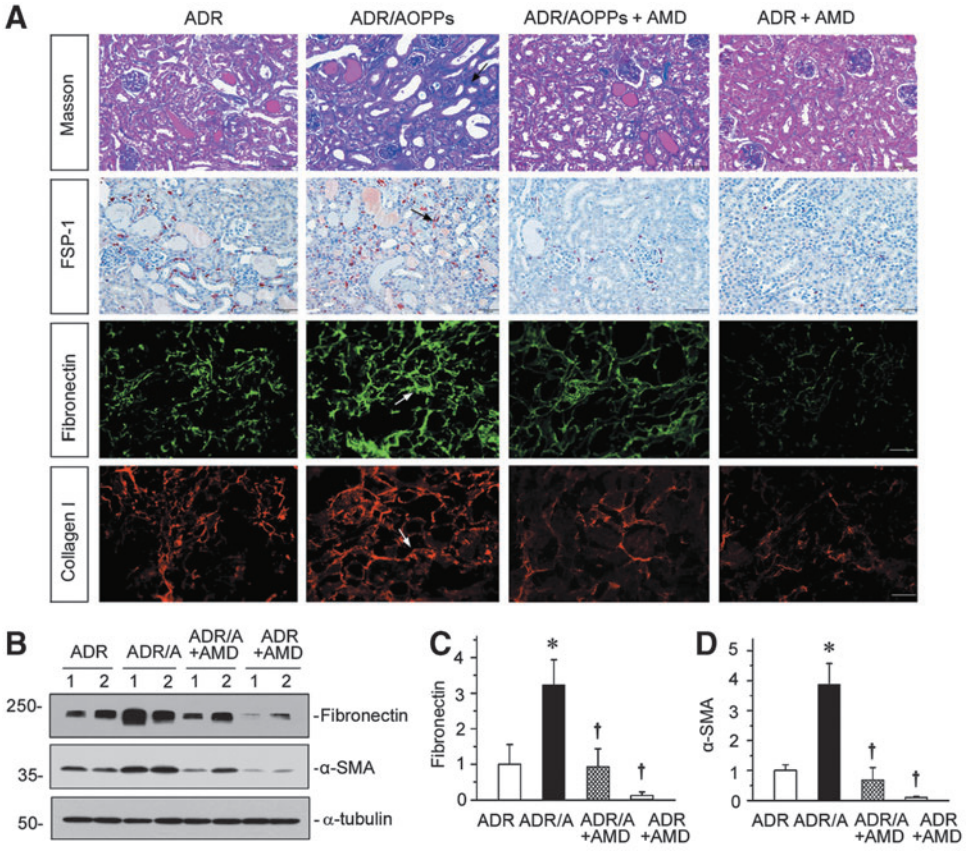

FIG. 6. AMD3100 inhibits AOPP-induced renal fibrosis in ADR nephropathy. (A) Representative images show Masson's trichrome staining, and immunohistochemical staining of FSP-1, and immunofluorescence staining of fibronectin and collagen I. *Arrows* indicate positive staining. Scale bar, 50 μm. **(B–D)** Western blotting analyses **(B)** and quantitative graphs of fibronectin **(C)** and α-SMA **(D)** in different groups. Numbers (1 and 2) represent different animals in a given group. $^{*}p < 0.05$ *versus* ADR group; $^{\dagger}p < 0.05$ *versus* ADR or ADR plus AOPPs vehicle controls ($n = 5$–6). All full unedited gels for Figure 6 are presented in Supplementary Figure S10.

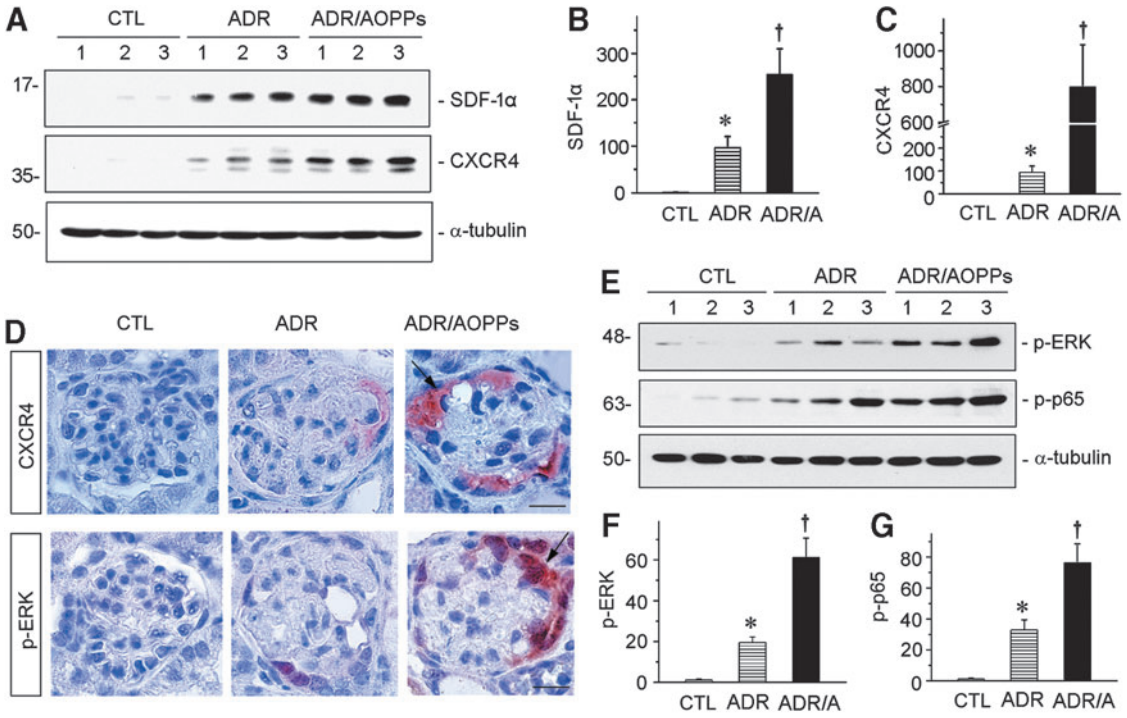

FIG. 7. AOPPs activates p-ERK/SDF-1α/CXCR4 pathway in ADR nephropathy. (A) Western blotting shows SDF-1α and CXCR4 protein expression in three groups as indicated. Numbers (1–3) represent different animals in a given group. **(B, C)** Quantitative graphs of SDF-1α **(B)** and CXCR4 **(C)** expressions in different groups. $^{*}p < 0.05$ *versus* normal controls; $^{\dagger}p < 0.05$ *versus* ADR alone ($n = 5$–6). **(D)** Representative images show CXCR4 and p-ERK expressions in podocytes in different groups as indicated. Scale bar, 20 μm. **(E)** Western blotting shows p-ERK and p-p65 protein expression in three groups as indicated. Numbers (1–3) represent different animals in a given group. **(F, G)** Quantitative graphs of p-ERK **(F)** and p-p65 **(G)** expressions in different groups. $^{*}p < 0.05$ *versus* normal controls; $^{\dagger}p < 0.05$ *versus* ADR alone ($n = 5$ to 6). All full unedited gels for Figure 7 are presented in Supplementary Figure S11. ERK, extracellular signal-regulated kinase; p-p65, phosphorylated NF-κB subunit p65; SDF-1α, stromal cell-derived factor 1α.

injections with ADR alone or ADR plus AOPPs. As shown in Figure 7E and F, phosphorylation of ERK was substantially induced in ADR nephropathy, which was further aggravated by AOPPs. Notably, both CXCR4 and p-ERK colocalized specifically in glomerular podocytes after injury (Fig. 7D, arrows), further supporting the notion that ERK activation may play a role in CXCR4 induction. Similarly, phosphorylated NF-κB subunit p65 (p-p65) was also induced in the kidneys after ADR injection, which was further promoted by AOPPs (Fig. 7E, G).

CXCR4 mediates AOPP-induced podocyte injury in vitro

To further confirm the role of CXCR4 in mediating oxidative stress-induced podocyte injury, we examined the regulation of SDF-1α/CXCR4 in cultured podocytes *in vitro*. To this end, mouse podocytes (MPC5) were treated with AOPPs for different periods. As illustrated in Figure 8A, AOPPs induced both SDF-1α and CXCR4 mRNA expression in cultured podocytes, as demonstrated by qRT-PCR. Western blotting and immunostaining also revealed that AOPPs induced CXCR4 protein expression (Fig. 8B–D). Of interest, CXCR4 predominantly localized in the nucleus (Fig. 8D), indicating its nuclear translocation after AOPPs treatment. Earlier studies suggest that nuclear translocation of CXCR4 is an integral part of its signaling and correlates with the progression of cancer (30, 42).

We found that SDF-1α could imitate AOPPs and triggered podocyte dedifferentiation and dysfunction, as evidenced by downregulation of podocyte-specific markers, such as WT1, nephrin, and podocalyxin (Fig. 8E, F), suggesting that activation of CXCR4 is sufficient to impair podocyte integrity and function. To further ascertain the role of CXCR4 in mediating podocyte injury, we tested whether the activation of CXCR4 signaling is required for AOPP-triggered podocyte dysfunction. As shown in Figure 8G, incubation of podocytes with AMD3100 mitigated the loss of WT1 and abolished the induction of desmin (Fig. 8G–I). Furthermore, knockdown of CXCR4 by small interfering RNA (siRNA) strategy resulted in significant downregulation of CXCR4 expression in podocytes (Supplementary Fig. S4) and mitigated the loss of podocalyxin and zona occludens 1 (ZO-1) in podocytes induced by AOPPs (Fig. 8J, K).

CXCR4 induction is dependent on activation of ERK and p65

We further studied the upstream signaling of CXCR4 in oxidative stress-induced podocyte injury by using cultured podocytes *in vitro*. As shown in Figure 9A–D, AOPPs induced phosphorylation and activation of both ERK and

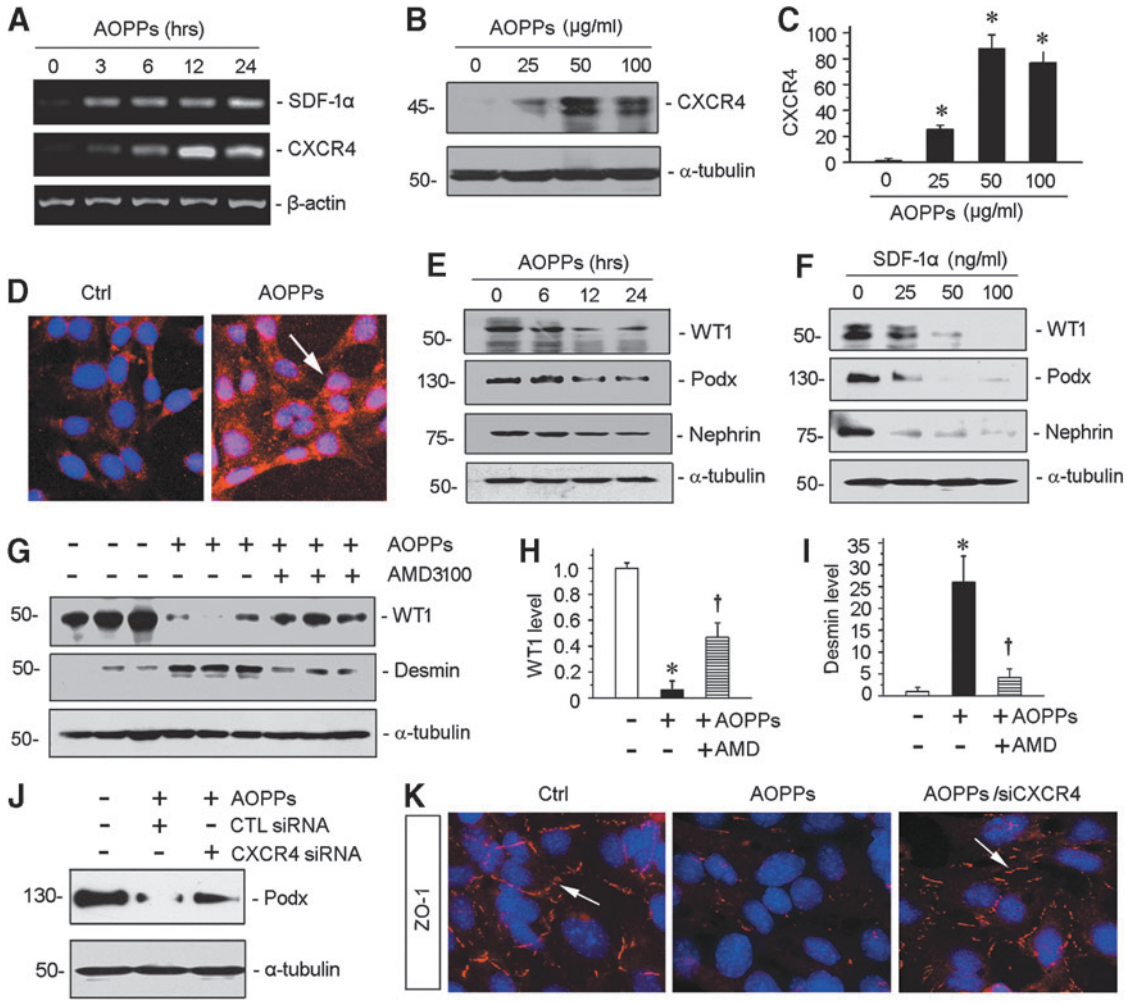

FIG. 8. CXCR4 mediates AOPP-induced podocyte injury. **(A)** Representative agarose gels show AOPP-induced SDF-1α/CXCR4 pathway in a time-dependent manner. **(B)** Western blotting shows AOPP-induced CXCR4 expression in cultured podocytes. Conditional immortal podocyte cell line (MPC5) was treated with AOPPs (0–100 μg/ml) for 12 h. Whole cell lysates were probed with CXCR4 antibody. **(C)** Graphical representations of the relative abundances of CXCR4 levels in four groups as indicated. *$p < 0.05$ *versus* medium alone ($n = 3$). **(D)** Immunofluorescence images show CXCR4 staining in cultured podocytes after treated with AOPPs. CXCR4 was increased by AOPPs and localized in nucleus. (**E**) Western blotting shows that AOPPs decreased WT1, podocalyxin (Podx), and nephrin expression in a time-dependent manner. MPC5 was treated with AOPPs at dose of 50 μg/ml at different times. **(F)** Western blotting shows that SDF-1α, ligand of CXCR4 receptor, depressed WT1, podocalyxin (Podx), and nephrin expression in a dose-dependent manner. MPC5 was treated with SDF-1α for 12 h. **(G)** Western blotting and quantitative analyses of WT1 **(H)** and desmin **(I)** in three groups as indicated. *$p < 0.05$ *versus* medium alone ($n = 3$); †$p < 0.05$ *versus* AOPPs alone ($n = 3$). **(J)** Western blotting shows that knockdown of CXCR4 reduced AOPP-induced podocyte injury. Podocytes were transfected with control or CXCR4-specific siRNA. Podocalyxin (Podx) protein expression was analyzed by Western blotting. **(K)** Representative images show ZO-1 staining. Knockdown of CXCR4 preserves tight junction marker ZO-1 in cell-cell contact. All full unedited gels for Figure 8 are presented in Supplementary Figure S12. MPC5, mouse podocytes; siRNA, small interfering RNA; ZO-1, zona occludens 1.

NF-κB p65 subunit in a time-dependent manner. After treatment with AOPPs, ERK phosphorylation in podocytes reached the peak at 15 min (Fig. 9B), while p65 phosphorylation was maximal at 60 min (Fig. 9D). Preincubation with U0126, a highly selective inhibitor of ERK upstream MEK1 and MEK2, significantly abolished the AOPP-induced p65 activation (Fig. 9E, F), suggesting that ERK is an upstream regulator of p65 activation. Similarly, blockade of ERK activation by U0126 abolished the AOPP-induced expression of CXCR4 and restored nephrin and WT1 expression (Fig. 9G–J). Furthermore, administration of SN50, a highly selective peptide inhibitor that blocks nuclear translocation of the NF-κB active complex, also largely blocked the induction of CXCR4 triggered by AOPPs (Fig. 9K, L). These data establish a critical role for ERK/p65 NF-κB signaling in mediating oxidative stress-triggered CXCR4 induction and podocyte injury.

CXCR4 mediates AOPP-induced NADPH oxidase activation in vitro

To further confirm the role of CXCR4 in mediating oxidative stress, we investigated NADPH oxidase activity

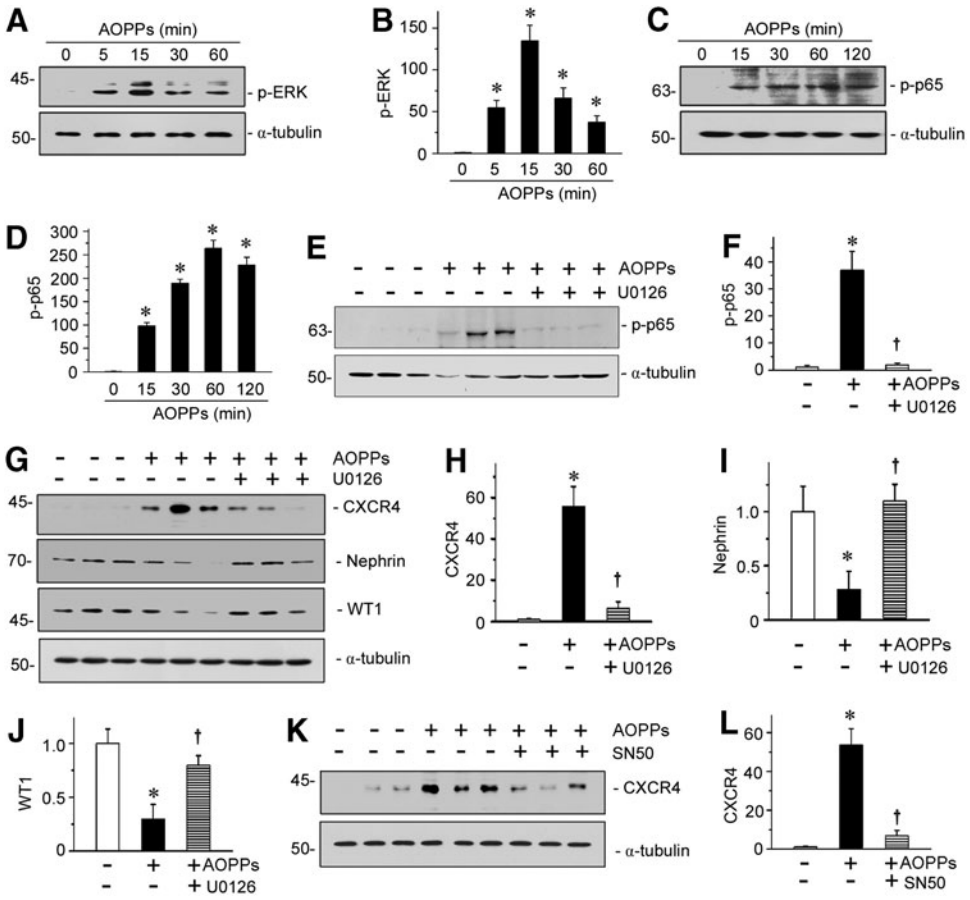

FIG. 9. CXCR4 mediates AOPP-induced podocyte injury through p-ERK/p-p65 activation. **(A)** Western blotting shows that AOPP-induced ERK phosphorylation in cultured podocytes. MPC5 cells were treated with AOPPs (50 μg/ml) for various periods as indicated. **(B)** Graphical representation of p-ERK abundances in different groups as indicated. $^{*}p < 0.05$ *versus* medium alone ($n = 3$). **(C)** Western blotting shows p65 phosphorylation in AOPP-induced MPC5 cells. **(D)** Graphical representation of p-p65 levels in different groups as indicated. $^{*}p < 0.05$ *versus* medium alone ($n = 3$). **(E, F)** Western blotting and graphical representation show that inhibition of ERK activation abolished AOPP-induced p65 phosphorylation in podocytes. $^{*}p < 0.05$ *versus* medium alone ($n = 3$). **(G)** Representative Western blotting shows that AOPPs induced upregulation of CXCR4 and downregulation of nephrin and WT1 in podocyte. U0126, a highly selective inhibitor of MAPK/ERK kinase, significantly reverses AOPP-induced CXCR4 upregulation and podocyte injury. MPC5 cell was pretreated with U0126 (10 μM) for 1 h, then treated with AOPPs at dose of 50 μg/ml for 12 h. **(H–J)** Quantitative analyses show CXCR4, nephrin, and WT1 expression in three groups. $^{*}p < 0.05$ *versus* medium alone ($n = 3$); $^{\dagger}p < 0.05$ *versus* AOPPs alone ($n = 3$). **(K)** Western blotting shows CXCR4 expression in medium alone, AOPPs, and AOPPs plus SN50 groups. The results show SN50, the specific NF-κB inhibitor, remarkably inhibited CXCR4 upregulation in AOPP-treated podocyte cell line. **(L)** Quantitative analysis of CXCR4 in three groups as indicated. $^{*}p < 0.05$ *versus* medium alone ($n = 3$); $^{\dagger}p < 0.05$ *versus* AOPPs alone ($n = 3$). All full unedited gels for Figure 9 are presented in Supplementary Figure S13. NF-κB, nuclear factor κB.

and ROS levels in AOPP-treated podocytes. As shown in Figure 10A–C, treatment of AOPPs further augmented the expression of p47phox and NOX4, the two key subunits of NAPDH oxidase (51, 54), in ADR-induced podocytes. We next examined the regulation of NOX4 after transfection with a Flag-tagged CXCR4 overexpression vector in cultured podocytes. As shown in Figure 10D, overexpression of CXCR4 markedly upregulated the expression of NOX4 in podocytes. Furthermore, we examined the phosphorylation of p47phox, the most critical step of NAPDH oxidase activation, by immunoprecipitation of p47phox and phosphoserine. As shown in Figure 10E, incubation of podocytes with AMD3100 inhibited the phosphorylation of p47phox, suggesting a critical role of CXCR4 in NAPDH oxidase activation. We next assessed the ROS production by 2,7-dichlorodihydrofluorescein diacetate (DCFH-DA) fluorescence. Blockade of CXCR4 by AMD3100 clearly abolished the ROS production by AOPPs (Fig. 10F). Similarly, AMD3100 also significantly inhibited the induction of both p47phox and NOX4 expression in AOPP-treated podocytes (Fig. 10G–I).

We also investigated the effect of NAPDH oxidase on CXCR4 expression in podocytes. To this end, podocytes were incubated with ADR in the presence or absence of apocynin, a specific NADPH oxidase inhibitor. We found that induction of CXCR4 by ADR was attenuated in the presence of apocynin (Supplementary Fig. S5), suggesting a reciprocal activation loop between CXCR4 and oxidative stress in podocyte injury (Fig. 10J).

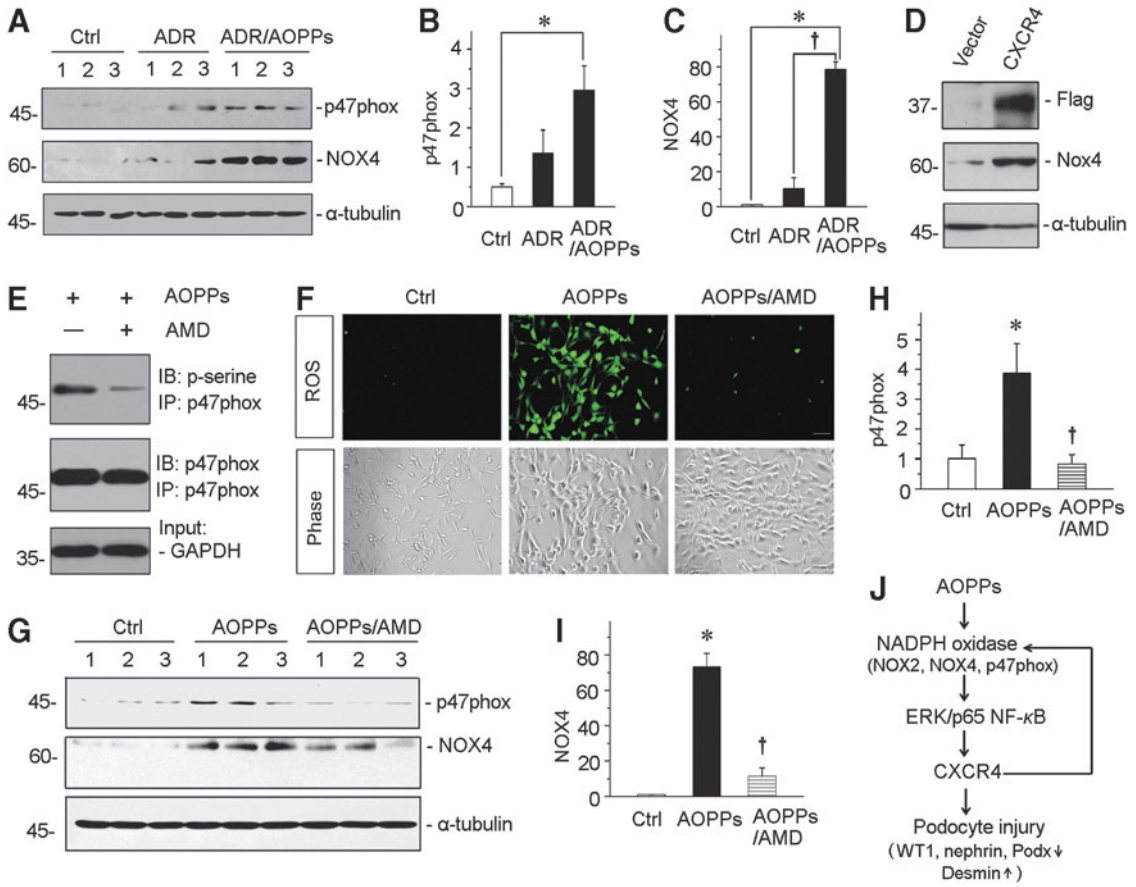

FIG. 10. CXCR4 mediates AOPP-induced NADPH oxidase activation *in vitro*. (A) Western blotting shows that AOPP-aggravated p47phox and NOX4 upregulation in ADR-treated podocytes. MPC5 cells were treated with ADR (1 μg/ml) alone or ADR with AOPPs (50 μg/ml) for 12 h. Whole cell lysates were analyzed by Western blotting. **(B, C)** Graphical representation of p47phox and NOX4 abundances in different groups as indicated. $^{*}p<0.05$ *versus* control ($n=3$). $^{\dagger}p<0.05$ *versus* ADR alone ($n=3$). **(D)** Western blotting shows that overexpression of CXCR4 promoted upregulation of NOX4. MPC5 cells were transfected with a Flag-tagged CXCR4 overexpression plasmid or empty vector for 24 h, and then, whole cell lysates were immunoblotted with antibodies against Flag, NOX4, and α-tubulin, respectively. **(E)** Coimmunoprecipitation demonstrates that AMD3100 inhibited the phosphorylation of p47phox. MPC5 cells were preincubated with AMD3100 (5 μg/ml) for 1 h and then treated with AOPPs (50 μg/ml) for 30 min. Cell lysates were immunoprecipitated with antibody against p47phox, followed by immunoblotting with anti-phosphoserine or anti-p47phox antibodies. **(F)** ROS production is induced by AOPPs in cultured podocytes but blocked by coincubation with AMD3100. MPC5 cells were treated with AOPPs or AOPPs plus AMD for 6 h. ROS production was assessed by detection of DCFH fluorescence (*green*). Cells were also observed with phase-contrast microscopy. Scale bar, 50 μm. **(G)** Representative Western blotting shows that AOPP-induced upregulations of p47phox and NOX4 were largely inhibited by AMD3100 in podocyte. MPC5 cells were preincubated with AMD3100 and then treated with AOPPs for 12 h. **(H, I)** Quantitative analyses show p47phox and NOX4 expressions in different groups as indicated. $^{*}p<0.05$ *versus* control ($n=3$); $^{\dagger}p<0.05$ *versus* AOPPs alone ($n=3$). **(J)** Schematic presentation of reciprocal activation loop between CXCR4 and oxidative stress in podocyte injury. All full unedited gels for Figure 10 are presented in Supplementary Figure S14. DCFH, 2,7-dichlorodihydrofluorescein; ROS, reactive oxygen species.

CXCR4 mediates AOPP-induced podocyte injury in glomerular miniorgan culture

To closely model podocytes *in vivo*, we used glomerular miniorgan culture, an *ex vivo* model system that largely preserves the sophisticated three dimensional architecture of podocytes in the kidney (40, 56). As shown in Figure 11A, rat glomeruli were isolated by differential sieving technique and cultured in suspension, which retained relatively intact glomerular structure. AOPPs significantly induced CXCR4 expression and inhibited nephrin in the glomerular miniorgan culture (Fig. 11B–D). Incubation with AMD3100 blocked CXCR4 induction by AOPPs and largely prevented the loss of nephrin (Fig. 11E–G). Similar results were obtained when nephrin and WT1 were detected by immunofluorescence staining (Fig. 11H).

Discussion

Oxidative stress is well known to be implicated in the pathogenesis of a variety of chronic diseases in multiple organs, including the kidney, liver, lung, and heart (27, 36, 43). In the kidney, podocytes are particularly vulnerable to the

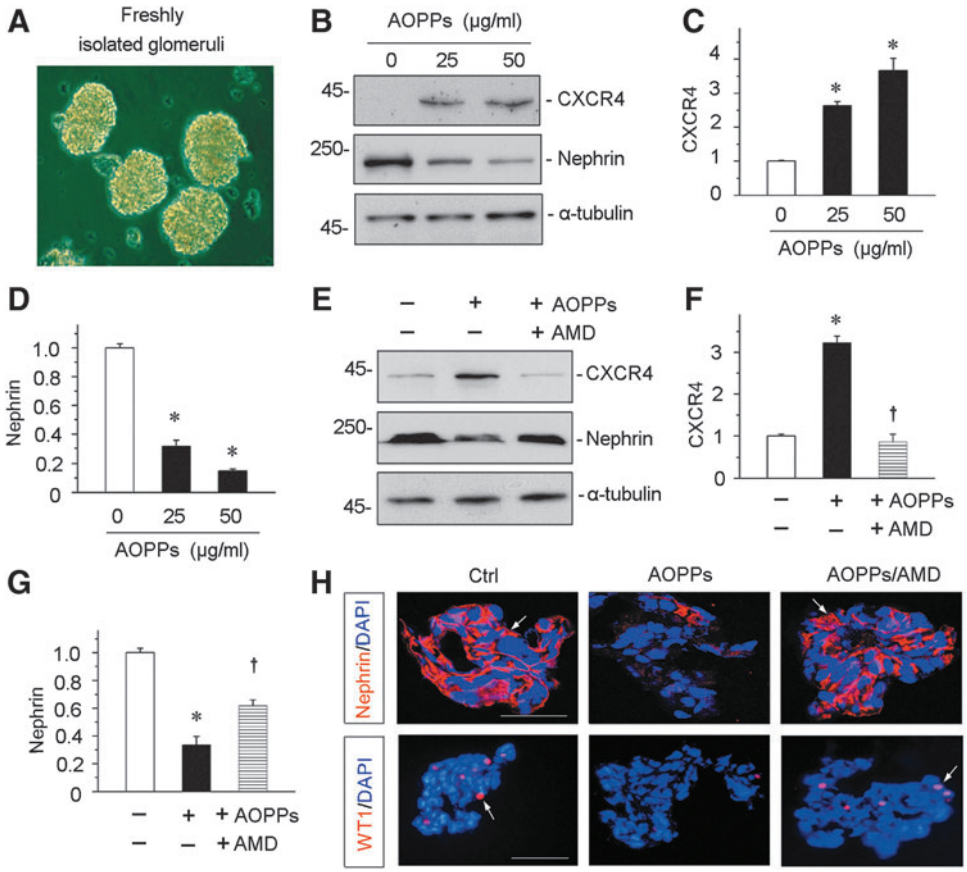

FIG. 11. CXCR4 mediates AOPP-induced podocyte injury in glomerular miniorgan culture. (A) Representative micrograph shows glomerular miniorgan culture *in vitro*. Glomeruli were isolated from rat kidneys and cultivated in suspension. **(B–D)** Western blotting shows that AOPPs induced CXCR4 upregulation and inhibited nephrin expression in cultured glomeruli. Rat glomeruli were treated with AOPPs (0–50 μg/ml) for 24 h. Quantitative analysis show CXCR4 **(C)** and nephrin **(D)** expression in different groups as indicated. $^{*}p < 0.05$ *versus* controls ($n = 3$). **(E–G)** Western blotting shows that AOPPs induced CXCR4 upregulation and suppressed nephrin expression, which were abolished by AMD3100 in cultured glomeruli. Rat glomeruli were pretreated with AMD3100 (5 μg/ml) for 1 h and then treated with AOPPs (50 μg/ml) for 24 h. Quantitative analyses show CXCR4 **(F)** and nephrin **(G)** expression in three groups. $^{*}p < 0.05$ *versus* controls ($n = 3$). $^{\dagger}p < 0.05$ *versus* AOPPs alone ($n = 3$). **(H)** Immunofluorescence staining shows that AOPPs inhibited expression of nephrin and WT1, which was abolished by AMD3100 in glomerular culture. *Arrows* indicate positive staining. Scale bar, 40 μm. All full unedited gels for Figure 11 are presented in Supplementary Figure S15.

damage caused by oxidative stress (1, 45), although it also triggers tubular injury, fibroblast activation, monocyte and macrophage recruitment, and mesangial cell proliferation (2, 43, 49). Extensive studies demonstrate that activation of numerous pathological signal pathways such as NADPH oxidase, transforming growth factor beta (TGF-β), renin-angiotensin system (RAS), and hypoxia-inducible factor-1 (HIF-1) is capable of triggering oxidative stress. However, how oxidative stress transmits its signal and causes podocyte damage remains to be elucidated. In this study, we demonstrate that activation of chemokine receptor CXCR4 signaling plays a crucial role in mediating oxidative stress-triggered podocyte injury and proteinuria. Our findings also underscore that CXCR4 could be a new target for mitigating podocyte injury, proteinuria, and glomerular sclerosis in proteinuric CKD.

Chemokines, a family of chemotactic cytokines, are 8–12 kDa peptides that serve as the chemoattractant to cell trafficking and adhesion. The biologic functions of chemokines are mediated by their specific receptors. As a G-protein-coupled seven-span transmembrane receptor, CXCR4 is specific and obligatory for chemokine SDF-1. The SDF-1/CXCR4 axis is reported to be involved in the pathogenesis of many disorders, such as stroke, tumor progression and metastasis, and angiogenesis (16, 18). It also plays a role in high glucose-mediated T cell activation (22) and ischemia-induced retinal neovascularization. Recent studies have begun to suggest its involvement in the development of various kidney disorders as well, such as acute kidney injury, and rapidly progressive glomerulonephritis (4, 7, 59).

One of the important findings in this study is the activation of CXCR4 receptor signaling in glomerular podocytes after ADR injury, a model of FSGS. Although the exact pathomechanisms of ADR nephrology remain unclear, generation of excessive ROS is believed to be a major culprit that triggers podocyte malfunction and damage (45). Interestingly, oxidative stress induced by ADR is associated with CXCR4 induction (Fig. 1 and Supplementary Fig. S5), suggesting that it may serve as an intermediate that links oxidative stress to podocyte damage. In ADR nephropathy and human kidney biopsies from patients with proteinuric kidney diseases,

CXCR4 was induced in podocytes and accompanied by an increased upregulation of oxidative stress, as illustrated by MDA assay, podocyte-specific nitrotyrosine staining, and induction of NOX2, NOX4, and p47phox, major subunits of NADPH oxidase (Figs. 2 and 10). The conclusion that oxidative stress mediates induction of CXCR4 is further supported by the results using AOPPs, a family of oxidized, dityrosine-containing protein products generated during excessive production of oxidants. Notably, AOPPs are able to induce both SDF-1α and CXCR4 expression in glomerular podocytes *in vivo* and *in vitro* (Figs. 7 and 8), suggesting a concurrent upregulation of this ligand/receptor axis. Consistently, nuclear translocation of CXCR4 is evident in AOPP-treated podocytes (Fig. 8), underscoring the functional activation of this signaling in podocytes. This observation is in harmony with a number of studies showing that CXCR4 nuclear localization determines disease severity and prognosis in cancer (30, 42).

Given the potential importance of CXCR4 in mediating oxidative stress-triggered podocyte injury, it is reasonable to speculate a role for CXCR4 antagonists in the treatment of proteinuric kidney diseases. Indeed, inhibition of CXCR4 by AMD3100, also known as plerixafor or Mozobil, a bicyclam molecule and a specific antagonist for CXCR4 and SDF-1-mediated chemotaxis with IC50 of 44 and 5.7 nM, respectively (6), is able to block proteinuria and ameliorates podocyte dysfunction and renal fibrotic lesions in ADR nephropathy (Figs. 5 and 6). AMD3100 has been shown to inhibit SDF-1-mediated GTP-binding, calcium flux, and chemotaxis but does not inhibit calcium flux against cells expressing CXCR3, CCR1, CCR2b, CCR4, CCR5, or CCR7 when stimulated with their cognate ligands, suggesting the specificity of its action. Previous studies also demonstrate that AMD3100 improves ischemia–reperfusion injury (IRI) and inflammation in rodent models of myocardial infarction, hind limb ischemia, and renal ischemia–reperfusion (19, 46). The mechanism underlying the beneficial effects of AMD3100 is related to its ability to modulate CXCR4-mediated leukocyte infiltration and the release of proinflammatory chemokines. The results in this study, for the first time, show that AMD3100 ameliorates glomerular sclerosis (Fig. 5) and renal fibrosis (Fig. 6) induced by oxidative stress. This observation is consistent with the fact that induction of CXCR4 occurs not only in glomerular podocytes but also in tubular epithelial cells as well (Fig. 1). AMD3100 not only preserves renal histology and inhibits the expression of fibrosis-related proteins (Fig. 6) but also restores podocyte SD-associated proteins, such as nephrin, podocalyxin, and ZO-1 (Figs. 5 and 8), as well as WT1, a zinc-finger transcription factor that is essential for the maintenance of the differentiated state of podocytes by promoting podocyte-specific gene expression (47). Therefore, these results indicate that the biological significance of CXCR4 upregulation in the presence of oxidative stress is podocyte dedifferentiation/dysfunction, and therefore, targeting CXCR4 signaling by AMD3100 could be an effective strategy for the prevention and treatment of proteinuric kidney diseases.

Our studies have also elucidated the mechanism by which oxidative stress upregulates CXCR4 expression in podocytes. Previous studies showed that CXCR4 expression is regulated by numerous growth factors and proinflammatory cytokines through their unique and specific pathways. For instance, galectin-1 is reported to induce CXCR4 expression by ERK/NF-κB-dependent pathway in renal cell carcinoma. In ovarian cancer, tumor necrosis factor alpha (TNF-α) upregulates CXCR4 expression *via* NF-κB signaling (21), while epidermal growth factor promotes CXCR4 expression through binding to its receptor and activating PI3K/Akt/mTOR signaling (35). In this study, we have uncovered that AOPPs activate ERK and p65 NF-κB signaling and blockade of these pathways abolishes CXCR4 expression in podocytes (Fig. 9), suggesting the potential role of MAPK and NF-κB signaling in oxidative stress-induced CXCR4 expression. Of note, AOPPs transmit its signaling *via* the receptor for advanced glycation endproduct (RAGE) (53), which directly binds to AOPPs and mediates its action in triggering ROS generation (53). The downstream of ROS is activation of ERK/NF-κB. It appears that ERK activation is the upstream event of p65 phosphorylation because the peak of ERK phosphorylation precedes the peak of p65 and inhibition of ERK activation abolishes p65 phosphorylation (Fig. 9). This conclusion is also supported by other earlier reports demonstrating that TNF-α induces CXCR4 by MAPK1/ERK1/2 signal pathway as well as the DNA binding of NF-κB (21, 29).

The present study uncovers an important role of CXCR4 in mediating oxidative stress-induced podocyte injury. Oxidative stress, triggered by ADR and/or AOPPs, induces NADPH oxidase activation and ROS generation, which stimulates ERK1/2 phosphorylation and nuclear translocation of p65 NF-κB (14). This cascade of events induces CXCR4 expression, leading to suppression of podocyte-specific proteins, such as WT1, nephrin, podocalyxin, and ZO-1, and induction of desmin. In turn, CXCR4 also induces NAPDH oxidase activation and production of ROS, thereby creating a vicious cycle of oxidative stress, CXCR4 induction, and podocyte injury (Fig. 10J). However, we cannot exclude the possibility that other pathways besides CXCR4 also play a role in mediating oxidative stress-induced podocyte dysfunction. The role and pathological contribution of tubular CXCR4 in the pathogenesis of oxidative stress-associated nephropathies remain to be determined. Another limitation of the present study is that the conclusion is largely based on a small-molecule inhibitor AMD3100 *in vivo*, which could have off-target effects. Future studies using genetic approach with podocyte-specific deletion of CXCR4 are needed.

In summary, we have shown that CXCR4 plays an important role in mediating oxidative stress-induced podocyte injury and proteinuria. CXCR4 is significantly upregulated in glomerular podocytes by oxidation through ERK/NF-κB pathway. Additionally, inhibition of CXCR4 is able to block oxidative stress, podocyte injury, and ameliorate glomerulosclerosis. This study provides a novel and mechanistic linkage between oxidative stress and podocyte damage in the pathogenesis of glomerulosclerosis. Although more studies are needed, these results provide a proof of principle that targeted inhibition of podocyte CXCR4 is able to protect podocytes against oxidative stress-triggered injury in proteinuric CKD.

Materials and Methods

Animal models

Mouse model of podocyte injury and proteinuria was established by intravenous injection of ADR, as described previously (48, 56). Male BALB/c mice weighing 22–24 g

were obtained from the Southern Medical University. Five groups of mice were used: (a) normal control ($n=5$); (b) ADR mice injected with vehicle ($n=6$); (c) ADR mice treated with AOPPs ($n=6$); (d) ADR mice treated with AOPPs and AMD 3100 ($n=6$); and (e) ADR mice treated with AMD 3100 ($n=6$). ADR (doxorubicin hydrochloride; Sigma, St. Louis, MO) was administrated by a single intravenous injection at 10.5 mg/kg body weight. AOPPs were injected at 100 mg/kg/d by tail injection. AMD3100 was dissolved in sterile saline and intraperitoneally injected at 1 mg/kg/d. The animals were sacrificed at the end of week 2. For the 5/6NX model, male CD-1 mice (23–25 g) were subjected to the surgical resection of the upper and lower poles, two thirds of the left kidney, or sham operation. One week later (week 0), the intact right kidney was removed *via* a right flank incision, as previously described (58). At week 6, all mice were euthanized and sacrificed. For Ang II infusion model, male C57Bl/6J mice weighing 22–24 g were infused with saline or Ang II (1.5 mg/kg/d) for 28 days. Urine and kidney tissue were collected for various analyses. All animal studies were performed by use of the procedures approved by compliance with the university's Guidelines for the Care and Use of Laboratory Animals.

AOPPs-MSA preparation

AOPPs-MSA was prepared *in vitro* by incubation of MSA (Sigma Chemical, St Louis, MO) with hypochlorous acid (Fluke, Buchs, Switzerland) in the absence of free amino acid/carbohydrates/lipids to exclude the formation of AGEs-like structures, as previously described (53, 54). Shortly, prepared samples were dialyzed against free hypochlorous acid and passed through a Detoxi-Gel column (Pierce, Rockford, IL) to remove contaminated endotoxin.

MDA, urinary albumin, creatinine, and 8-OHdG assay

MDA was detected by commercial kits (Cayman Chemical Company, Ann Arbor, MI). Briefly, the kidney cortex tissues were homogenized and used for measurements according to the manufacturer's protocol. Kidney cortex MDA was normalized by total protein contents for each tissue and expressed as μmol/μg pro. Urine albumin was measured by using a mouse Albumin ELISA Quantitation kit, according to the manufacturer's protocol (Bethyl Laboratories, Inc., Montgomery, TX). Urinary and serum creatinine levels were determined by use of a QuantiChrom creatinine assay kit (DICT-500; Bioassay Systems, Hayward, CA), according to the manufacturer's protocols. Urinary albumin was standardized to urine creatinine and expressed as mg/mg Ucr. Urinary 8-OHdG level was analyzed by a commercial ELISA kit (CEA660Ge; USCN Life Science, Inc., Wuhan, China) and equilibrated by urine creatinine.

Histology and immunohistochemical staining

Paraffin-embedded mouse kidney sections (3 μm thickness) were prepared by a routine procedure. Sections were stained with hematoxylin–eosin, PAS reagent, and MTS for assessing collagen deposition and fibrotic lesions by standard procedure. The extent of glomerular sclerosis was assessed by a semiquantitative analysis using the method of Raij *et al.* (37): grade 0, no mesangial expansion and glomerular hypertrophy of glomerulus; grade 1, mesangial expansion and glomerular hypertrophy of glomerulus of up to 25%; grade 2, mesangial expansion and glomerular hypertrophy of glomerulus of 25%–50%; grade 3, mesangial expansion and glomerular hypertrophy of glomerulus of 50%–75%; grade 4, mesangial expansion and glomerular hypertrophy of glomerulus of 75%–100%. At least 50 glomeruli were evaluated under $\times 400$ magnification and results averaged for each kidney. The sclerosis index for each mouse was calculated as follows: $(N1\times 1+N2\times 2+N3\times 3+N4\times 4)/n$, where N1, N2, N3, and N4 represent the numbers of glomeruli that exhibited grades 1, 2, 3, and 4, respectively, and n represents the number of glomeruli assessed. Quantification of the fibrotic area was carried out by a computer-aided point-counting technique, as described previously (50, 58). Immunohistochemical staining was performed using routine protocol. The following antibodies were used: rabbit anti-CXCR4 (sc-9046 and sc-6190; Santa Cruz Biotechnology, Santa Cruz, CA), rabbit anti-fibronectin (F3648; Sigma), rabbit anti-α-SMA (ab5694; Abcam, Cambridge, MA), rabbit polyclonal anti-FSP-1(S100A4) (A5114; DAKO, Carpinteria, CA), rabbit anti-desmin (PB0095; Boster, Wuhan, China), and rabbit anti-phospho-p44/42 MAPK (ERK1/2) (Thr202/Tyr204) (9101; Cell Signaling Technology, Danvers, MA). Some sections were also stained with anti-AOPPs mAb (Clone 3F2). The primary anti-AOPPs mAb was produced by our laboratory and has been demonstrated to react specifically with hypochlorous acid-modified proteins but not with the native form or other oxidant-modified proteins (26).

Immunofluorescence staining and confocal microscopy

Kidney cryosections or cells cultured on coverslips were fixed with 3.7% paraformaldehyde for 15 min at room temperature. After blocking with 10% donkey serum for 30 min, the slides were immunostained with primary antibodies against nitrotyrosin (SAB5200009; Sigma), α-actinin-4 (ALX-210–356-C050; Enzo Life Sciences, Farmingdale, NY), collagen I (BA0325, Boster), nephrin (20R-NP002; Fitzgerald Industries International, Concord, MA), WT1 (sc-192; Santa Cruz Biotechnology), podocalyxin (AF1556; R&D Systems, Minneapolis, MN), fibronectin (F3648; Sigma), CXCR4 (Abcam), and ZO-1 (61–7300; Thermo Fisher Scientific, Waltham, MA).

Western blot analysis

Protein expression was analyzed by Western blot analysis, as described previously (55). The primary antibodies used were as follows: anti-CXCR4 (ab2074; Abcam), anti-nephrin (ab58968; Abcam), anti-nephrin (Fitzgerald Industries International), anti-desmin (Boster), fibronectin (Sigma), anti-α-SMA (A2547; Sigma), anti-MMP-7 (GTX104658; GeneTex, Irvine, CA), anti-podocalyxin (AF1556; R&D Systems), anti-SDF-1α (ab25117; Abcam), anti-phospho-ERK (Cell Signaling Technology), anti-phospho-NF-kB p65 (Ser536) (3036; Cell Signaling Technology), anti-WT1 (Santa Cruz Biotechnology), anti-flag (F4042; Sigma-Aldrich), anti-p47phox (07-500, Thermo Fisher Scientific), anti-NOX4 (BA2813; Boster), anti-p-serine (BM1622; Boster), anti-CXCR7 (SAB2700198; Sigma), anti-α-tubulin (RM2007; Rayantibody, Beijing, China), and anti-GAPDH (BM1623; Boster).

Intracellular production of ROS

Intracellular ROS was detected in podocytes by analyzing the fluorescence intensity of the intracellular fluoroprobe DCFH (10 μM) after the incubation of AOPPs at indicated time. Representative images obtained by fluorescent microscopy (Leica DMi8).

Glomerular miniorgan culture

Glomeruli were isolated by differential sieving technique from male Sprague Dawley rats (Harlan Sprague Dawley), as previously reported (56). Briefly, kidneys were excised and pressed with a spatula through stainless steel screens through differential sieves (60, 100, and 200 meshes) and collected for cultivation. The purity of glomeruli was about 95% using this approach. Isolated glomeruli were cultured in RPMI1640/10% fetal bovine serum (FBS) medium at 37°C on noncoated six-well plates in the absence or presence of AOPPs or AOPPs plus AMD3100.

Immunoprecipitation

The phosphorylation of p47phox was detected by immunoprecipitation, as described previously (54). Briefly, the cell lysates were preabsorbed with protein A/G agarose beads (sc-2003; Santa Cruz Biotechnology) and incubated with a polyclonal rabbit anti-p47phox antibody (Santa Cruz Biotechnology). The immunocomplexes were blotted with mouse monoclonal anti-p-serine antibody (BM1622; Boster) or p47phox antibody.

Real-time reverse transcriptase (RT)-PCR

Total RNA isolation and quantitative RT-PCR or real-time RT-PCR (qRT-PCR) were carried out by a routine procedure. Briefly, first-strand complementary DNA (cDNA) synthesis was carried out using the Reverse Transcription System kit according to the manufacturer's instructions (Promega, Madison, WI). Real-time RT-PCR was performed on ABI PRISM 7000 Sequence Detection System (Applied Biosystems, Foster City, CA). The PCR mixture is in a 25 μl volume containing 12.5 μl 2 × SYBR Green PCR Master Mix (Applied Biosystems), 5 μl diluted RT product (1:10), and 0.5 μM sense and antisense primer sets. The sequences of the primer pairs used in RT-PCR or qRT-PCR were as follows: mouse NOX2, 5′-GGGAACTGGGCTGTGAATGA-3′ and 5′-CAG TGCTGACCCAAGGAGTT-3′; mouse NOX4, 5′-CCATGC CTTCTTACTGTGTCCT-3′ and 5′-GAGTGACTCCAATG CCTCCA-3′; mouse CXCR4, 5′-TGGAACCGATCAGTGT GAGT-3′ and 5′-CGGTACTTGTCCGTCATGCT-3′; mouse Podocalyxin, 5′-GCTTTCTCCTAAGGCCGTGT-3′ and 5′-ACAAGGAGCAGGAAGGATGC-3′; mouse SDF-1α, 5′-AGAAAGCTTTAAACAAGGGGCG-3′ and 5′-TTACAAA GCGCCAGAGCAGA-3′; mouse glyceraldehyde-3-phosphate dehydrogenase, 5′-CCAATGTGTCCGTCGTGGAT-3′ and 5′-TGCTGTTGAAGTCGCAGGAG-3′; and mouse β-actin, 5′-CAGCTGAGAGGGAAATCGTG-3′ and 5′-CGTTGCC AATAGTGATGACC-3′. PCR was run by using standard conditions. Real-time PCR was performed using a Platinum SYBR Green qPCR SuperMix-UDG kit (Invitrogen, Carlsbad, CA). After sequential incubations at 50°C for 2 min and 95°C for 10 min, respectively, the amplification protocol consisted of 50 cycles of denaturing at 95°C for 15 s, and annealing and extension at 60°C for 60 s. The standard curve was made from series dilutions of template cDNA. The mRNA levels of various genes were calculated after normalizing with GAPDH or β-actin.

Cell culture and treatment

The conditionally immortalized mouse podocyte cell line (MPC5) was provided by Peter Mundel (Massachusetts General Hospital, Boston, MA) and maintained, as described previously (53). To propagate podocytes, cells were cultured at 33°C in RPMI1640 medium supplemented with 10% FBS and 10 U/ml mouse recombinant interferon gamma (IFN-γ; R&D Systems) to enhance the expression of a thermosensitive T antigen. To induce differentiation, podocytes were grown under nonpermissive conditions at 37°C in the absence of IFN-γ. MPC5 cells were treated with AOPPs and SDF-1α (SRP-4388; Sigma) at indicated doses and time. For some experiments, MPC5 cells were pretreated with CXCR4 inhibitor AMD3100 (A5602; Sigma) at 5 μg/ml, and MAPK/ERK kinase inhibitor U0126 (9903; Cell Signaling Technology) and NF-κB p65 subunit translocation inhibitor SN50 (ALX-167-024-C500; Enzo Life Sciences) were pretreated for 1 h, followed by incubation with AOPPs. Whole-cell lysates were prepared and subjected to Western blot analyses. Some cells were plated on sterile coverslips for detection of immunofluorescence. For some studies, podocytes were transiently transfected with flag-tagged CXCR4 expression vector (pCMV-CXCR4) or control and CXCR4-specific siRNA (sc-35422; Santa Cruz Biotechnology) as indicated by using Lipofectamine 2000 reagent (Invitrogen).

Statistical analyses

All data examined were expressed as mean ± standard error of the mean. Statistical analysis of the data was carried out using SPSS 13.0, (SPSS, Inc., Chicago, IL). Comparison between groups was made using one-way analysis of variance (ANOVA) followed by Student–Newman–Keuls test or Dunnett's T3 procedure. A p value of <0.05 was considered significant.

Acknowledgments

This work was presented in the First International Congress of Chinese Nephrologists, held in Hong Kong, China, December 11–13, 2015. The abstract was published in the proceeding of that meeting (Mo H, Hong X, Zhou L, and Liu Y. CXCR4 plays a crucial role in mediating oxidative stress-induced podocyte injury. *Hong Kong J Nephrol* 17 (2 Suppl.): S77, 2015). This work was supported by National Natural Science Foundation of China grants 81370014, 81521003, and 81570620, Guangdong Science Foundation grant 2014A030312014, and Guangzhou Projects grant 201504010001. L.Z. was also supported by the Foundation for Distinguished Young Talents in Higher Education of Guangdong, China (LYM10043) and the Foundation for the Author of Excellent Doctoral Dissertation of Guangdong, China (sybzzxm201223).

Author Disclosure Statement

No competing financial interest exists.

References

1. Abe Y, Sakairi T, Beeson C, and Kopp JB. TGF-β1 stimulates mitochondrial oxidative phosphorylation and generation of reactive oxygen species in cultured mouse podocytes, mediated in part by the mTOR pathway. *Am J Physiol Renal Physiol* 305: F1477–F1490, 2013.
2. Bondi CD, Manickam N, Lee DY, Block K, Gorin Y, Abboud HE, and Barnes JL. NAD(P)H oxidase mediates TGF-beta1-induced activation of kidney myofibroblasts. *J Am Soc Nephrol* 21: 93–102, 2010.
3. Camilla R, Suzuki H, Dapra V, Loiacono E, Peruzzi L, Amore A, Ghiggeri GM, Mazzucco G, Scolari F, Gharavi AG, Appel GB, Troyanov S, Novak J, Julian BA, and Coppo R. Oxidative stress and galactose-deficient IgA1 as markers of progression in IgA nephropathy. *Clin J Am Soc Nephrol* 6: 1903–1911, 2011.
4. Chong BF and Mohan C. Targeting the CXCR4/CXCL12 axis in systemic lupus erythematosus. *Expert Opin Ther Targets* 13: 1147–1153, 2009.
5. Dai C, Stolz DB, Kiss LP, Monga SP, Holzman LB, and Liu Y. Wnt/beta-catenin signaling promotes podocyte dysfunction and albuminuria. *J Am Soc Nephrol* 20: 1997–2008, 2009.
6. De Clercq E. AMD3100/CXCR4 inhibitor. *Front Immunol* 6: 276, 2015.
7. Ding M, Cui S, Li C, Jothy S, Haase V, Steer BM, Marsden PA, Pippin J, Shankland S, Rastaldi MP, Cohen CD, Kretzler M, and Quaggin SE. Loss of the tumor suppressor Vhlh leads to upregulation of Cxcr4 and rapidly progressive glomerulonephritis in mice. *Nat Med* 12: 1081–1087, 2006.
8. Doring Y, Pawig L, Weber C, and Noels H. The CXCL12/CXCR4 chemokine ligand/receptor axis in cardiovascular disease. *Front Physiol* 5: 212, 2014.
9. Eid AA, Gorin Y, Fagg BM, Maalouf R, Barnes JL, Block K, and Abboud HE. Mechanisms of podocyte injury in diabetes: role of cytochrome P450 and NADPH oxidases. *Diabetes* 58: 1201–1211, 2009.
10. Fornoni A, Jeon J, Varona Santos J, Cobianchi L, Jauregui A, Inverardi L, Mandic SA, Bark C, Johnson K, McNamara G, Pileggi A, Molano RD, Reiser J, Tryggvason K, Kerjaschki D, Berggren PO, Mundel P, and Ricordi C. Nephrin is expressed on the surface of insulin vesicles and facilitates glucose-stimulated insulin release. *Diabetes* 59: 190–199, 2010.
11. Fukuda R, Suico MA, Kai Y, Omachi K, Motomura K, Koga T, Komohara Y, Koyama K, Yokota T, Taura M, Shuto T, and Kai H. Podocyte p53 limits the severity of experimental alport syndrome. *J Am Soc Nephrol* 27: 144–157, 2016.
12. Grahammer F, Schell C, and Huber TB. The podocyte slit diaphragm—from a thin grey line to a complex signalling hub. *Nat Rev Nephrol* 9: 587–598, 2013.
13. Guo J, Ananthakrishnan R, Qu W, Lu Y, Reiniger N, Zeng S, Ma W, Rosario R, Yan SF, Ramasamy R, D'Agati V, and Schmidt AM. RAGE mediates podocyte injury in adriamycin-induced glomerulosclerosis. *J Am Soc Nephrol* 19: 961–972, 2008.
14. Guo ZJ, Niu HX, Hou FF, Zhang L, Fu N, Nagai R, Lu X, Chen BH, Shan YX, Tian JW, Nagaraj RH, Xie D, and Zhang X. Advanced oxidation protein products activate vascular endothelial cells via a RAGE-mediated signaling pathway. *Antioxid Redox Signal* 10: 1699–1712, 2008
15. Huang CY, Lee CY, Chen MY, Yang WH, Chen YH, Chang CH, Hsu HC, Fong YC, and Tang CH. Stromal cell-derived factor-1/CXCR4 enhanced motility of human osteosarcoma cells involves MEK1/2, ERK and NF-kappaB-dependent pathways. *J Cell Physiol* 221: 204–212, 2009.
16. Huang J, Li Y, Tang Y, Tang G, Yang GY, and Wang Y. CXCR4 antagonist AMD3100 protects blood-brain barrier integrity and reduces inflammatory response after focal ischemia in mice. *Stroke* 44: 190–197, 2013.
17. Jefferson JA and Shankland SJ. The pathogenesis of focal segmental glomerulosclerosis. *Adv Chronic Kidney Dis* 21: 408–416, 2014.
18. Jujo K, Hamada H, Iwakura A, Thorne T, Sekiguchi H, Clarke T, Ito A, Misener S, Tanaka T, Klyachko E, Kobayashi K, Tongers J, Roncalli J, Tsurumi Y, Hagiwara N, and Losordo DW. CXCR4 blockade augments bone marrow progenitor cell recruitment to the neovasculature and reduces mortality after myocardial infarction. *Proc Natl Acad Sci U S A* 107: 11008–11013, 2010.
19. Jujo K, Ii M, Sekiguchi H, Klyachko E, Misener S, Tanaka T, Tongers J, Roncalli J, Renault MA, Thorne T, Ito A, Clarke T, Kamide C, Tsurumi Y, Hagiwara N, Qin G, Asahi M, and Losordo DW. CXC-chemokine receptor 4 antagonist AMD3100 promotes cardiac functional recovery after ischemia/reperfusion injury via endothelial nitric oxide synthase-dependent mechanism. *Circulation* 127: 63–73, 2013.
20. Koshikawa M, Mukoyama M, Mori K, Suganami T, Sawai K, Yoshioka T, Nagae T, Yokoi H, Kawachi H, Shimizu F, Sugawara A, and Nakao K. Role of p38 mitogen-activated protein kinase activation in podocyte injury and proteinuria in experimental nephrotic syndrome. *J Am Soc Nephrol* 16: 2690–2701, 2005.
21. Kulbe H, Hagemann T, Szlosarek PW, Balkwill FR, and Wilson JL. The inflammatory cytokine tumor necrosis factor-alpha regulates chemokine receptor expression on ovarian cancer cells. *Cancer Res* 65: 10355–10362, 2005.
22. Lan X, Cheng K, Chandel N, Lederman R, Jhaveri A, Husain M, Malhotra A, and Singhal PC. High glucose enhances HIV entry into T cells through upregulation of CXCR4. *J Leukoc Biol* 94: 769–777, 2013.
23. Levoye A, Balabanian K, Baleux F, Bachelerie F, and Lagane B. CXCR7 heterodimerizes with CXCR4 and regulates CXCL12-mediated G protein signaling. *Blood* 113: 6085–6093, 2009.
24. Li HY, Hou FF, Zhang X, Chen PY, Liu SX, Feng JX, Liu ZQ, Shan YX, Wang GB, Zhou ZM, Tian JW, and Xie D. Advanced oxidation protein products accelerate renal fibrosis in a remnant kidney model. *J Am Soc Nephrol* 18: 528–538, 2007.
25. Lin CH, Shih CH, Tseng CC, Yu CC, Tsai YJ, Bien MY, and Chen BC. CXCL12 induces connective tissue growth factor expression in human lung fibroblasts through the Rac1/ERK, JNK, and AP-1 pathways. *PLoS One* 9: e104746, 2014.
26. Liu B, Hou X, Zhou Q, Tian J, Zhu P, Xu J, Hou F, and Fu N. Detection of advanced oxidation protein products in patients with chronic kidney disease by a novel monoclonal antibody. *Free Radic Res* 45: 662–671, 2011.
27. Liu SX, Hou FF, Guo ZJ, Nagai R, Zhang WR, Liu ZQ, Zhou ZM, Zhou M, Xie D, Wang GB, and Zhang X. Advanced oxidation protein products accelerate atherosclerosis

through promoting oxidative stress and inflammation. *Arterioscler Thromb Vasc Biol* 26: 1156–1162, 2006.
28. Lotan D, Sheinberg N, Kopolovic J, and Dekel B. Expression of SDF-1/CXCR4 in injured human kidneys. *Pediatr Nephrol* 23: 71–77, 2008.
29. Maroni P, Bendinelli P, Matteucci E, and Desiderio MA. HGF induces CXCR4 and CXCL12-mediated tumor invasion through Ets1 and NF-kappaB. *Carcinogenesis* 28: 267–279, 2007.
30. Masuda T, Nakashima Y, Ando K, Yoshinaga K, Saeki H, Oki E, Morita M, Oda Y, and Maehara Y. Nuclear expression of chemokine receptor CXCR4 indicates poorer prognosis in gastric cancer. *Anticancer Res* 34: 6397–6403, 2014.
31. Nagasawa T. CXCL12/SDF-1 and CXCR4. *Front Immunol* 6: 301, 2015.
32. Nielsen JS and McNagny KM. The role of podocalyxin in health and disease. *J Am Soc Nephrol* 20: 1669–1676, 2009.
33. O'Boyle G, Swidenbank I, Marshall H, Barker CE, Armstrong J, White SA, Fricker SP, Plummer R, Wright M, and Lovat PE. Inhibition of CXCR4-CXCL12 chemotaxis in melanoma by AMD11070. *Br J Cancer* 108: 1634–1640, 2013.
34. Pavenstadt H, Kriz W, and Kretzler M. Cell biology of the glomerular podocyte. *Physiol Rev* 83: 253–307, 2003.
35. Phillips RJ, Mestas J, Gharaee-Kermani M, Burdick MD, Sica A, Belperio JA, Keane MP, and Strieter RM. Epidermal growth factor and hypoxia-induced expression of CXC chemokine receptor 4 on non-small cell lung cancer cells is regulated by the phosphatidylinositol 3-kinase/PTEN/AKT/mammalian target of rapamycin signaling pathway and activation of hypoxia inducible factor-1alpha. *J Biol Chem* 280: 22473–22481, 2005.
36. Planavila A, Redondo-Angulo I, Ribas F, Garrabou G, Casademont J, Giralt M, and Villarroya F. Fibroblast growth factor 21 protects the heart from oxidative stress. *Cardiovasc Res* 106: 19–31, 2015.
37. Raij L, Azar S, and Keane WF. Role of hypertension in progressive glomerular immune injury. *Hypertension* 7: 398–404, 1985.
38. Rehman AO and Wang CY. SDF-1alpha promotes invasion of head and neck squamous cell carcinoma by activating NF-kappaB. *J Biol Chem* 283: 19888–19894, 2008.
39. Schwartzman M, Reginensi A, Wong JS, Basgen JM, Meliambro K, Nicholas SB, D'Agati V, McNeill H, and Campbell KN. Podocyte-specific deletion of Yes-associated protein causes FSGS and progressive renal failure. *J Am Soc Nephrol* 27: 216–226, 2016.
40. Sheikh BN, Bechtel-Walz W, Lucci J, Karpiuk O, Hild I, Hartleben B, Vornweg J, Helmstädter M, Sahyoun AH, Bhardwaj V, Stehle T, Diehl S, Kretz O, Voss AK, Thomas T, Manke T, Huber TB, and Akhtar A. MOF maintains transcriptional programs regulating cellular stress response. *Oncogene* 35: 2698–2710, 2016.
41. Shibata S, Nagase M, Yoshida S, Kawachi H, and Fujita T. Podocyte as the target for aldosterone: roles of oxidative stress and Sgk1. *Hypertension* 49: 355–364, 2007.
42. Speetjens FM, Liefers GJ, Korbee CJ, Mesker WE, van de Velde CJ, van Vlierberghe RL, Morreau H, Tollenaar RA, and Kuppen PJ. Nuclear localization of CXCR4 determines prognosis for colorectal cancer patients. *Cancer Microenviron* 2: 1–7, 2009.
43. Stokman G, Qin Y, Booij TH, Ramaiahgari S, Lacombe M, Dolman ME, van Dorenmalen KM, Teske GJ, Florquin S, Schwede F, van de Water B, Kok RJ, and Price LS. Epac-Rap signaling reduces oxidative stress in the tubular epithelium. *J Am Soc Nephrol* 25: 1474–1485, 2014.
44. Susztak K, Raff AC, Schiffer M, and Böttinger EP. Glucose-induced reactive oxygen species cause apoptosis of podocytes and podocyte depletion at the onset of diabetic nephropathy. *Diabetes* 55: 225–233, 2006.
45. Tan RJ, Zhou D, Xiao L, Zhou L, Li Y, Bastacky SI, Oury TD, and Liu Y. Extracellular superoxide dismutase protects against proteinuric kidney disease. *J Am Soc Nephrol* 26: 2447–2459, 2015.
46. Tan Y, Li Y, Xiao J, Shao H, Ding C, Arteel GE, Webster KA, Yan J, Yu H, Cai L, and Li X. A novel CXCR4 antagonist derived from human SDF-1beta enhances angiogenesis in ischaemic mice. *Cardiovasc Res* 82: 513–521, 2009.
47. Wagner N, Wagner KD, Xing Y, Scholz H, and Schedl A. The major podocyte protein nephrin is transcriptionally activated by the Wilms' tumor suppressor WT1. *J Am Soc Nephrol* 15: 3044–3051, 2004.
48. Wang Y, Wang YP, Tay YC, and Harris DC. Progressive adriamycin nephropathy in mice: sequence of histologic and immunohistochemical events. *Kidney Int* 58: 1797–1804, 2000.
49. Wei XF, Zhou QG, Hou FF, Liu BY, and Liang M. Advanced oxidation protein products induce mesangial cell perturbation through PKC-dependent activation of NADPH oxidase. *Am J Physiol Renal Physiol* 296: F427–F437, 2009.
50. Xiao L, Zhou D, Tan RJ, Fu H, Zhou L, Hou FF, and Liu Y. Sustained activation of Wnt/β-catenin signaling drives AKI to CKD progression. *J Am Soc Nephrol* 27: 1727–1740, 2016.
51. You YH, Quach T, Saito R, Pham J, and Sharma K. Metabolomics reveals a key role for fumarate in mediating the effects of NADPH oxidase 4 in diabetic kidney disease. *J Am Soc Nephrol* 27: 466–481, 2016.
52. Zheng S, Carlson EC, Yang L, Kralik PM, Huang Y, and Epstein PN. Podocyte-specific overexpression of the antioxidant metallothionein reduces diabetic nephropathy. *J Am Soc Nephrol* 19: 2077–2085, 2008.
53. Zhou LL, Cao W, Xie C, Tian J, Zhou Z, Zhou Q, Zhu P, Li A, Liu Y, Miyata T, Hou FF, and Nie J. The receptor of advanced glycation end products plays a central role in advanced oxidation protein products-induced podocyte apoptosis. *Kidney Int* 82: 759–770, 2012.
54. Zhou LL, Hou FF, Wang GB, Yang F, Xie D, Wang YP, and Tian JW. Accumulation of advanced oxidation protein products induces podocyte apoptosis and deletion through NADPH-dependent mechanisms. *Kidney Int* 76: 1148–1160, 2009.
55. Zhou L, Li Y, Hao S, Zhou D, Tan RJ, Nie J, Hou FF, Kahn M, and Liu Y. Multiple genes of the renin-angiotensin system are novel targets of Wnt/β-catenin signaling. *J Am Soc Nephrol* 26: 107–120, 2015.
56. Zhou L, Li Y, He W, Zhou D, Tan RJ, Nie J, Hou FF, and Liu Y. Mutual antagonism of Wilms' tumor 1 and β-catenin dictates podocyte health and disease. *J Am Soc Nephrol* 26: 677–691, 2015.
57. Zhou L and Liu Y. Wnt/β-catenin signalling and podocyte dysfunction in proteinuric kidney disease. *Nat Rev Nephrol* 11: 535–545, 2015.
58. Zhou L, Mo H, Miao J, Zhou D, Tan RJ, Hou FF, and Liu Y. Klotho ameliorates kidney injury and fibrosis and nor-

malizes blood pressure by targeting the renin-angiotensin system. *Am J Pathol* 185: 3211–3223, 2015.
59. Zuk A, Gershenovich M, Ivanova Y, MacFarland RT, Fricker SP, and Ledbetter S. CXCR(4)antagonism as a therapeutic approach to prevent acute kidney injury. *Am J Physiol Renal Physiol* 307: F783–F797, 2014.

Address correspondence to:
Dr. Lili Zhou
State Key Laboratory of Organ Failure Research
National Clinical Research Center of Kidney Disease
Division of Nephrology
Nanfang Hospital
Southern Medical University
Guangzhou 510515
China

E-mail: jinli730@smu.edu.cn

Prof. Youhua Liu
Department of Pathology
University of Pittsburgh School of Medicine
200 Lothrop Street
Pittsburgh, PA 15261

E-mail: liuy@upmc.edu

Date of first submission to ARS Central, May 24, 2016; date of final revised submission, December 8, 2016; date of acceptance, December 12, 2016.

Abbreviations Used

5/6NX = 5/6 nephrectomy
8-OHdG = 8-hydroxy-2′-deoxyguanosine
α-SMA = α-smooth muscle actin
ADR = adriamycin nephropathy
AOPPs = advanced oxidation protein products
cDNA = complementary DNA
CKD = chronic kidney disease
CXCR4 = C-X-C chemokine receptor type 4
CXCR7 = C-X-C chemokine receptor type 7
DCFH-DA = 2,7-dichlorodihydrofluorescein diacetate
ELISA = enzyme-linked immunosorbent assay
ERK = extracellular signal-regulated kinase
FBS = fetal bovine serum
FSGS = focal segmental glomerulosclerosis
Fsp-1 = fibroblast-specific protein 1
IFN-γ = interferon gamma
IgAN = immunoglobulin A nephropathy
MDA = malondialdehyde
MMP-7 = matrix metalloproteinase-7
MPC5 = mouse podocytes
mRNA = messenger RNA
MTS = Masson's trichrome staining
NF-κB = nuclear factor κB
PAS = Periodic acid-Schiff
p-p65 = phosphorylated NF-κB subunit p65
qRT-PCR = real-time RT-PCR
ROS = reactive oxygen species
SD = slit diaphragm
SDF-1α = stromal cell-derived factor 1α
siRNA = small interfering RNA
TNF-α = tumor necrosis factor alpha
WT1 = Wilms tumor 1
ZO-1 = zona occludens 1